

A
Dissertation Report on
**AC Grid Connected PV System with
Autonomous Operation**

Submitted
in partial fulfilment of the requirements for the degree of
Master of Technology
in
Electrical Power System

by
Mr. Patil Jaydeep Jaysing
(Roll No. 1729003)

Sponsored by
Sharad Electrical and Contractor, Sangli

Under the Supervision of
Mr. Chandrakant L. Bhattar



Department of Electrical Engineering
K.E. Society's
Rajarambapu Institute of Technology, Rajaramnagar
(An Autonomous Institute, Affiliated to Shivaji University, Kolhapur)
2018-2019

K.E. Society's

Rajarambapu Institute of Technology, Rajaramnagar

(An Autonomous Institute, Affiliated to Shivaji University, Kolhapur)

CERTIFICATE

This is to certify that, Mr. Jaydeep Jaysing Patil (Roll No- 1729003) has successfully completed the dissertation work and submitted dissertation report on "AC Grid Connected PV System with Autonomous Operation" for the partial fulfillment of the requirement for the degree of Master of Technology in Electrical Power System from the Department of Electrical Engineering, as per the rules and regulations of Rajarambapu Institute of Technology, Rajaramnagar, Dist: Sangli.

Date:

Place: RIT, Rajaramnagar

Mr. Chandrakant L. Bhattar

Mr Santosh T. Patil

Name and Sign of Supervisor

Name and Sign of Industrial Supervisor

Name

Dr. H. T. Jadhav

Name and Sign of External Examiner

Name and Sign of Head of Program

Dr. V. N. Kalkhambkar

Dr. Sharad D. Patil

Name and Sign of Head of Department

Name and Sign of PG Convener

DECLARATION

I declare that this report reflects my thoughts about the subject in my own words. I have sufficiently cited and referenced the original sources, referred or considered in this work. I have not misrepresented or fabricated or falsified any idea/data/fact/source in this my submission. I understand that any violation of the above will be cause for disciplinary action by the Institute.

Place: RIT, Rajaramnagar

Name of Student: Mr. Jaydeep J. Patil

Date:

Roll No: 1729003

ACKNOWLEDGEMENTS

I must mention several individuals and organizations that were of enormous help in the development of this work. Prof. Chandrakant L. Bhattar, my supervisor, philosopher and personality with a midas touch encouraged me to carry this work. His continuous invaluable knowledgeable guidance throughout the course of this study helped me to complete the work up to this stage and hope will continue in further research.

I also very thankful to HoP, HoD for their valuable suggestions, critical examination of work during the progress, I am indebted to them.

I am very grateful to Mr. Anil P. Yadav for his positive cooperation and immense kindly help during the period of work with him.

In addition, very energetic and competitive atmosphere of the Electrical Engineering Department had much to do with this work. I acknowledge with thanks to faculty, teaching and non-teaching staff of the department, Central library and Colleagues.

I sincerely thank to Mrs. S.S.Kulkarni, for supporting me to do this work and I am very much obliged to her.

Last but not the least; Mr. Jaysing Patil, my father, my mother, constantly supported me for this work in all aspects

Place: RIT, Rajaramnagar

Mr. Jaydeep J. Patil

Date:

Roll No:1729003

ABSTRACT

This paper presents the distribution AC grid is connected to photovoltaic system is based on voltage and frequency control strategy. Magnitude and speed are controlled at point of common coupling (PCC) using voltage –frequency control strategy in autonomous mode and p-q control strategy in grid connected mode. The PCC space vector is the comparison of the reference space vector that is simultaneously applied towards the PCC to extract the disturbance. The V(Q)-F(P) control strategy provide the active and reactive power generate, in response to voltage and frequency deviation. The voltage and frequency control strategy are applicable for single and three phase converter interfaced with energy system.

Keywords: p-q control strategy, autonomous (islanding detection) mode, Point of common coupling (PCC) space vector.

Contents

<i>CERTIFICATE</i>	ii
<i>SPONSORSHIP CERTIFICATE</i>	iii
<i>DECLARATION</i>	iv
<i>ACKNOWLEDGEMENTS</i>	v
<i>ABSTRACT</i>	vi
<i>CONTENT</i>	vii
<i>LIST OF FIGURES</i>	xi
<i>LIST OF TABLES</i>	xii
<i>NOMENCLATURE</i>	xiii
<i>ABBREVIATIONS</i>	xiii
1 Introduction	1
1.1 General	1
1.2 Motivation of the present work	3
1.3 Layout of the thesis	4
1.4 Closure	5
2 Literature Review	6
2.1 Introduction	6
2.2 Literature review	6
2.3 Objectives of present work	9
2.4 Closure	10
3 System Description	11
3.1 Introduction	11
3.2 PV Solar System	12
3.2.1 PV Cell Basic Concept	12

3.2.2	Modeling of PV cell	14
3.2.3	I-V and P-V Characteristics	16
3.2.4	Concept MPPT	19
3.2.5	Mathematical modeling of MPPT (Incremental Conduction Algorithm)	21
3.3	DC-DC coverter	22
3.4	DC-AC Inverter	25
3.5	Closure	28
4	Methodology	29
4.1	Introduction	29
4.2	V-F and P-Q Control Strategy	30
4.2.1	PQ control mode	30
4.2.2	VF control mode	32
4.3	Control loops	34
4.4	Mathematical Modeling	36
4.4.1	The Complete Control Structure of V(Q) and F(P) Strategy	36
4.5	Mode of Operation	39
4.6	Closure	40
5	Results and Discussion	41
5.1	Introduction	41
5.2	Simulation and results	41
5.3	Hardware and results	45
5.3.1	Hardware setup	45
5.3.2	Hardware Results	51
5.4	Comparison	54
5.5	Closure	56
6	Future scope and Conclusion	57
6.1	Conclusion	57
6.2	Future Scope	58
	<i>REFERENCES</i>	59
	<i>LIST OF PUBLICATIONS ON PRESENT WORK</i>	62
	<i>APPROVED COPY OF SYNOPSIS</i>	63

VITAE (CV) 70

List of Figures

3.1	Block Diagram of Proposed Work	12
3.2	PV effect converts the photon energy into voltage across the PN junction	13
3.3	Ideal PV Cell	14
3.4	Series Resistance	15
3.5	Shunt Resistance	15
3.6	Equivalent circuit of solar cell	16
3.7	I-V characteristics for light condition	17
3.8	I-V characteristics for no light condition	17
3.9	Irradiance is increase by the PV	18
3.10	I-V curve for solar cell to get the maximum output for solar cell	18
3.11	I-V curve for PV system with oprating point	19
3.12	I-V and PV curves show maximum power point from PV modules	20
3.13	I-V and PV curves show maximum power from PV modules in load line is shifted in left side	20
3.14	I-V and PV curves show maximum power from PV modules in load line is shifted in right side	21
3.15	Boost Converter	22
3.16	Mode I Switch is closed	23
3.17	Mode II Switch is open	23
3.18	Three phase inverter	26
3.19	Output Wave Form of Inverter	27
3.20	Inverter using IC CD4047	28
4.1	Inner current control loop	32
4.2	outer voltage loop	33

4.3	Equivalent Circuit For Emulating The Control Using Voltage Controlled Source	36
4.4	The Complete Control Structure	38
4.5	Position of Grid At Instant Transfer From Autonomous Mode To Grid Connected Mode	40
5.1	Simulation Model of PV System In Autonomous Operation	42
5.2	PV Voltage and Current	42
5.3	Boost converter output	43
5.4	Simulation Waveform For i_d i_q ref For Control Strategy	43
5.5	Simulation Waveform For i_d i_q PCC For Control Strategy	44
5.6	Simulation Waveform Inverter	44
5.7	Autonomous mode grid voltage Vab and grid current Ia	45
5.8	Autonomous mode grid voltage Vab and grid current Ia	45
5.9	PV Module	46
5.10	SMPS transformer	48
5.11	IC 4047	49
5.12	MOSFET	50
5.13	Prototype model	52
5.14	PV voltage and current	52
5.15	Boost converter output voltage	53
5.16	Inverter circuit output Voltage	53
5.17	Injected voltage in grid connected mode Vab Autonomous voltage	54

List of Tables

5.1 Comparison Table	55
--------------------------------	----

ABBREVIATIONS

PV	Photo Voltaic
PQ	Active (P)/Reactive(Q) Power
EES	Electrical Energy Source
MPPT	Maximum Power Point Tracking
MG	Micro Grid
SMPS	Switched Mode Poweer Supply
DC	Direct Current
AC	Alternating Current
VSI	Voltage Source Inverter
DG	Distribution Grid

Chapter 1

Introduction

1.1 General

The global energy crisis and the threat of disruption of the environment have become a common problem worldwide. Electricity demand is constantly increasing. Traditional sources of energy, such as heat, etc., have serious problems with limited reservoirs, which could end in the next few decades. Carbon emissions from conventional power plants pose a serious threat to the environment. Other energy sources. Nuclear power plants are seriously endangered for human safety.

To overcome the above concerns, researchers in recent years have been paying close attention to renewable energy sources of all renewable energy sources, solar energy is the most viable solution because it is available in abundance and for free around the world. Solar photovoltaic (PV) is used to convert solar energy to electricity. A complete solar energy conversion system consists of a solar photovoltaic system, electronic energy converters and control units for adjusting the power extracted from solar energy. Solar photovoltaic cells do not specify characteristics. Its efficiency is relatively low, and the power of the exact moment varies with respect to the solar system and the ambient temperature [2].

In order to obtain the highest possible energy from solar power under environmental conditions, the operation has to be repaired. In order to accomplish this task, several approaches have been proposed as the highest power monitoring (MPPT) [1]. The main plans are character development, Speed and Observe, constant voltage, and more. All of these plans have their own advantages and disadvantages as described in this sections.

The MPPT scheme is expected to improve under intermediate conditions, as it adds more than one peak to the PV feature. Apart from improving the MPPP algorithms under the classification of many other proposed methods such as PV module modules, layouts, electric power transformers to make changes to topology and other features are provided. it operates at high efficiency [5]. Electric power generators play a critical role in converting and regulating the power of solar PV as required. Various types of topologies namely one step, two step conversion and other factors have been proposed.

Distributed generation systems are designed to power AC grids within certain voltage and frequency limits. The main grid connection requirements for renewable electricity networks relate to the low-voltage and medium-voltage grids. The new generation power converters should be equipped with network support functions that work in concert when controlling island protection, voltage and frequency transients, and monitoring active / reactive power in case of network failures [21]. Grid code requirements typically refer to one active function at a time. Requirements include: Response to a frequency change to reduce active power for increased frequency and increase active power for low frequency. For example, a power generator should reduce its active power by a certain power gradient when the line frequency rises above a specified value. Support for a static network where the power generator must have custom reactive power settings. Power factor (PF) or reactive power (Q) is set to a constant value, reactive power value is a function of the voltage change of the network, $Q(v)$, The power factor is variable, with active power operation, $\cos \theta (P)$. Dynamic grid support (for example, passage through low and high voltage), at which the power generator generates reactive current along a predetermined transition voltage profile [21].

Renewable energy and electricity storage power are connected through the network by distributing the power of converters. The power supply can be used in the (off-grid) AC and connected to the line. Various approaches can be found for driving the electric field through various control techniques. The program manager can be designed to meet a wide range of three-phase and three-phase applications, including at least one of the following operational design templates:

- Grid-forming stand-alone (ups mode)
- Grid-supporting (islanded mode and grid-connected)

- Grid-feeding (grid-connected)
- Grid-loading (charge mode)

In support mode, the controller is designed to test the converter with integrated voltage- and current source and is commonly used in microgrids. The main purpose of the controller is to participate in voltage and frequency by controlling the operating power P and operating power Q provided from the converter. Controller-based control between homogeneous individuals in a microgrid system has been implemented using both the slab and the high voltage output. The low-voltage microgrid is supported in terms of voltage reduction using the P / V -droop feature to control the power output depending on the voltage range [32]. Optimal methods for the inverse relationship between countries and systems integration have been proposed in this section [9].

The proposed user-specific application is based on the new PV / wind generation model, which involves the durability of the integrated power supply network Integrated $P(f) - Q(v)$ auxiliary support networks. : Frequency- and frequency-assisted responses to signals of uncertainty. The data of $P(f) - Q(v)$ simulate the inverse / inertial capacitance equations for convergence in the direction of instantaneous output voltage and voltage associated with the switch Of PV / wind.

The support structures $P(f)$ and $Q(v)$ are implemented and integrated in the EES direction of the converter with the power transfer between the EES and the amplifier. The proposed methods can be implemented in the EES converters used in the power transformer and rechargeable electrodes, due to the common power supply and the direct current. The auxiliary control controller is suitable for low voltage, medium and high voltage. Customer well-being is the adaptation of the manager's attributes (for example, frameworks and arrangements for ongoing assistance and assistance in implementing strategies $P(f) - Q(v)$ and power management,) and balancing power with all applications. in mechanical engineering and telecommunications.

1.2 Motivation of the present work

Due to the increased penetration of distribution generation resources in microgrids, concerns about the interaction between the power systems have increased. The

microgrid can operate both in network connection mode and in standby mode, which increases the reliability and quality of electricity. When connected, the voltage and frequency of the micro-network are controlled by the main network. On the other hand, autonomous condition. All distributors must be engaged in maintaining voltage and frequency while sharing power output. It should also be integrated with a controller that adjusts its operating power so that the total power output is equal to the total loss. Because the distribution of power between the power source circuitry is an important factor for comparison, each module of the study was studied on a microgrid sequenced in the master control method.

1.3 Layout of the thesis

Based on the thesis work objectives, flow of dissertation work is divided into the Following chapters:

1. Chapter 1: A brief introduction to the photovoltaic system DC-DC converter and the research objectives are addressed in this chapter.
2. Chapter 2: The literature on the PV system, the DC-DC pulse converter and the VF / PQ control strategy are discussed in this chapter. All the published documents about the system, the DC-DC pulse converter and the VF / PQ control strategy are discussed in uniform and varied conditions.
3. Chapter 3: The description of the proposed system is discussed in this chapter. This includes a detailed description of the system, DC-DC pulse converter and VF / PQ control strategy.
4. Chapter 4: The operation and implementation of the VF / PQ control strategy are discussed in this chapter. It consists in modeling the proposed system. The design and operation of all circuits with their components and features used in hardware are discussed.
5. Chapter 5: Simulation and hardware results are described in this chapter. Comparison of various methods, such as voltage and frequency control, as well as methods for monitoring active and reactive power with the proposed control method, is presented. It also consists of the experimental hardware configuration of the proposed system and its results.
6. Chapter 6: Conclusion and future scope are described in this chapter.

1.4 Closure

In this section, the introduction about grid connected mode, autonomous mode, and their different control strategy like V-F and P-Q control strategy . Along with that, motivation of presented work and layout thesis are given.

Chapter 2

Literature Review

2.1 Introduction

This chapter consists of a detailed literature review of the various autonomous operations or Islanding operations used so far. Several schemes of control are proposed, which are used by several authors in the PQ and VF control strategy. This section contains a brief summary of all these research documents.

2.2 Literature review

Efstratios I. Batzeliis proposed “Simple PV Performance Equations Theoretically Well Founded on the Single-Diode Model” Below we present a new model of photovoltaic efficiency consisting of simple expressions for calculating Short Circuit, Open Circuit and MPP work points at each irradiation and temperature. The proposed equations have a solid theoretical basis and adapt very well to the model of a single diode. The required input data is always specified in the module technical data sheet. This makes the model generally applicable to all photovoltaic modules in the crystalline model. [1]

Yousef Mahmoud and Ehab El-Saadany prposed “Accuracy Improvement of the Ideal PV Model” Here ideal PV Proposes an effective approach to increase the accuracy of the model. Proposed approach low quality caution to ideal PV Improves the accuracy of the model, without compromising its simplicity. Measurements from manufacturer’s data sheets have been confirmed and the effectiveness of the proposed modeling method confirmed. [2]

Weidong Xiao, Fonkwe Fongang Edwin, Giovanni Spagnuolo, Juri Jatskevich,

“Efficient Approaches for Modeling and Simulating Photovoltaic Power Systems” This document is obvious and simple model for models that are appropriate for long-term and expensive extensions by PV improvements. The study provides a simple PV model and its measurement to ensure the characteristics of I-V are the data contained in the data store. A second phase power plug that is connected to the phase-link DC link is connected to a inverter string and a phase convert to the special PV export. [3]

B. Chitti Babu and Suresh Gurjar proposed “A Novel Simplified Two-Diode Model of Photovoltaic (PV) Module” Here novel modeling approach for PV modules using an ideal two-diode model. By omitting series and shunt resistors, this model is greatly simplified and at the same time, a comparable accuracy with less computational effort is achieved. Furthermore, it can be seen that the simulation results are very close to the values provided by the PV producers. To match the IV characteristic to the experimental curve, the ideality constants are accurately estimated with a simple iterative method. Consequently, the proposed study can contribute to the development of new photovoltaic systems, reducing costs and time. It can also be used to better understand its performance. [4]

Anonio Manuel Santos Spencer Andrede, Luciano Schuch, and Lucio da Silva martins, “Analysis and design of high efficiency hybrid High step up DC-DC converter for distributed PV generations system” has proposed a new high voltage increase of hybrid DC / DC converter designed by the connection of the standard boost converter with a coupled inductor and other power consuming guidelines. The invitation inverter is a challenge with an amendment that does not require much work. It accomplishes high voltage gain and high level of efficiency. [5]

Farzad Mohammmd zadeh Shahir, Ebrahim Babei, Murtuza Farsadi “Extended Topology for Boost DC-DC Converter” has suggested that the DC-DC converter non-inverted boost produce a high voltage boost but the conventional non-inverted DC-DC converter. Voltage and elimination of current balance and voltage increase in steady-state mode (Continuous Conduction Mode) and non-contiguous line mode (Dis-Continuous Conduction Mode) are extracted. The high voltage output is a general structure based on the DC-DC converter. [6]

Xu-Feng Chang, Yong Zhang, and Chengliang Yin “A Family of Coupled Inductor based Soft-Switching DC/DC Converter with Double Synchronous Recti-

fication” This article proposes a family of new, non-isolated, DC / DC converters with switched inductance that change the position of the coupled induction coil. These new DC / DC converters have similar properties but different mathematical descriptions to existing similar DC / DC converters with soft switching. To improve the performance of this type of DC / DC coupled transducers based on induction coils, including existing transducers, all of these coupled DC / DC converter based on induction coils use the existing efficiency improvement technique (used in Buck type converters) used. [7]

Guzmán Díaz, Cristina González-Morán, Javier Gómez-Aleixandre , Javier Gómez-Aleixandre “Complex-Valued State Matrices for Simple Representation of Large Autonomous Microgrids Supplied by PQ and VF Generation” This paper focuses on state-space representation The model of a micrograph in which power is regulated (PQ) and voltage-Frequency (VF) generating units share a distribution system. The generating units considered in this article are connected to the inverter. It presents some interesting models of modeling Problems that are treated in the paper such as cascade decoupling control loops or network dynamics that is not negligible. Methodology for modeling and stabilizing a large micro-network for small signal analysis. [8]

N. Hajilu, G.B. Gharehpetian, S.H. Hosseinian, M. R. Poursistani M. Kohansal “Power Control Strategy in Islanded Microgrids Based on VF and PQ Theory Using Droop Control of Inverters” this power supply (VSI) inverter can be operated in active reactive mode (PQ), active power supply mode (PV mode), and voltage frequency (VF mode) mode. The Micro Grid operation is influenced by the selection of the operator control strategy. Thus, in this study two typical checks The VSI schemes (PQ and VF) are generally explained and the Network for Active / Reactive Power is split between the right VSIs. In this control strategy, the power regulation for all VSIs should cover the total GG needs so that the PG power of the DGs is measured at the MPP and the VF DGs divide the remaining power after the strategy Droop control. The simulation results are displayed to confirm the proposed control strategy. [9]

Shan S. and Loganathan Umanand “A Unified controller for utility interactive uninterruptible power converters for grid connected and Autonomous operations” UIUPC to switch from a p-q control strategy in the grid connected mode to a

voltage-frequency control strategy in autonomous mode and vice versa. In this work, the concept for controlling the perturbation in size and velocity of the common coupling space vector was derived. The PCC space vector is compared to the reference space currently being applied toward the PCC space vector to extract the disturbance. The reference system of the proposed controller is linked to the dynamics of the PCC space vector. [10]

Soha Mansour, Mostafa I. Marei, Ahmed A. Sattar “Decentralized Secondary Control for Frequency Restoration of Microgrids with VF and PQ Droop Controlled Inverters” This paper introduces a distributed secondary control scheme for a micro-network (MG) containing VF and PQ regulated inverters. The proposed secondary controllers are based on identical PI controllers to generate the corresponding frequency offset compensation signals. The secondary controller action is used to change the Primary Controller Reference Controller, local to each DG unit. This static positioning active The mechanism will reset the system frequency to the nominal value. VF drives change their frequency setpoint PQ change their active power reference in proportion to the frequency error. Therefore, all inverters assume the. Part frequency recovery while keeping the power-sharing rate active thus avoids device overload and reliable and safe operation. [11]

Sarina Adhikari, and Fangxing Li, “Coordinated V-f and P-Q Control of Solar Photovoltaic Generators With MPPT and Battery Storage in Microgrids” This document was prepared jointly and in conjunction with Management of solar PV electricity with multiple Power Supply (MPPT) and Battery Management for Voltage and Frequency (VF) for a grid. Also, Active and Reactive (P-Q) with Sunlight Communications network, PV, MPPT and battery storage solutions. Strategic Ideas are a collaborative effort between Inverter V-F control or P-Q control, MPPT control and power storage Loading and downloading. The document also shows that good collaboration between the service providers is involved in the change of the changes in the company and the state of the battery (SOC). [12]

2.3 Objectives of present work

In this dissertation worked Grid Connected PV system with Autonomous operation mode, in this mode grid connected to autonomous mode and vice versa, this mode will carried out in MATLAB software.

1. To analyze p-q control strategy in grid connected mode and voltage-frequency control strategy in autonomous mode.
2. To Design non isolating DC-DC boost converter and PWM phase shift controller
3. To simulate and analyze model of proposed method in MATLAB SIMULINK environment.
4. To develop prototype for proposed method.

2.4 Closure

After a survey of the above literature of Autonomous or Islanding operation, it is noted that there are different control strategies used for improve the system performance. The different control strategy is used by researchers. The merits and demerits of mentioned control techniques are also discussed in the above literature.

Chapter 3

System Description

3.1 Introduction

Limited fossil energy and increased air pollution have spurred researchers to develop clean energy sources. One of these sources is the photovoltaic (PV) power generation system, which is a clean, quiet and an efficient method for generating electricity. In practical applications, PV arrays can be used in battery charging, water pumping, PV vehicles, satellite power systems, grid-connected power systems, standalone power systems, and so on. Due to the low conversion efficiency of PV arrays, one way to reduce the cost of the overall system is by using high efficiency power processors. The power processor usually adopts a dc/dc converter as its energy processing system. When a dc/dc converter is used in a PV array power system, it is operated at the maximum power point (MPP) of the PV arrays to extract the maximum possible power for increasing the utilization rate of the PV arrays. As a result, its output voltage does not remain at the desired constant dc voltage. Therefore, a dc/dc converter with voltage regulation is used to connect with PV power systems in parallel to keep the output voltage in the desired constant dc voltage range, as shown in fig 3.1.

The dc bus voltage can supply a dc/ac inverter for a grid-connected power system, a dc/dc converter for dc load, and so on. The dc/ac inverter and dc/dc converter are regarded as dc loads. In this paper, the proposed power supply includes a dc/dc converter as the maximum power point tracking (MPPT) point of the PV arrays and a dc/dc converter as the load voltage regulator. To increase the utility rate of PV arrays, power systems using PV arrays must track MPP

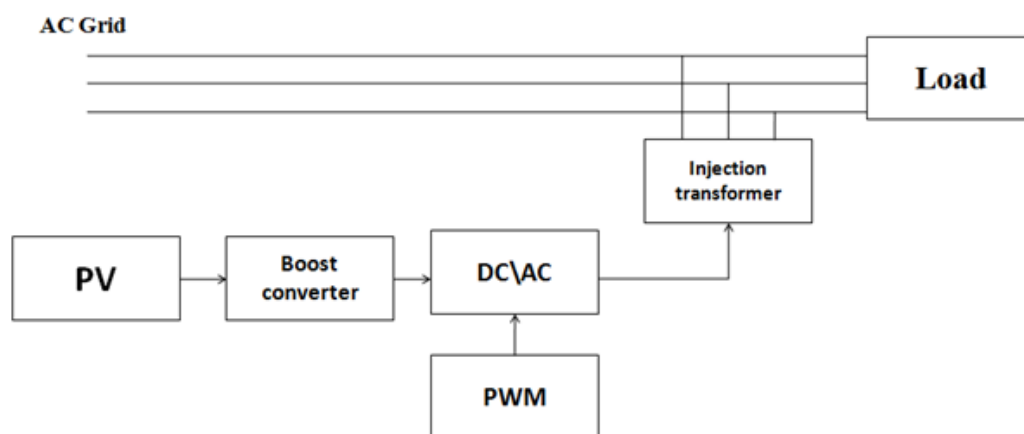


Figure 3.1: Block Diagram of Proposed Work

to extract as much power as possible from the arrays. Several MPPT algorithms have been proposed. Some of the more popular MPPT algorithms are the constant voltage method, β method, system oscillation method, ripple correlation method, incremental conductance method and perturb and observe method. Due to its simplicity and ease of implementation, the perturb and observe method is often used. Therefore, the perturb and observe method was adopted to implement the MPPT of the proposed power system.

3.2 PV Solar System

The main objective of PV modules is to generate DC current and voltage. For feeding electricity to grid, there are needed to convert these generated DC values into corresponding AC values. We know that the device which converts DC values into AC, which is called as an inverter. Furthermore, they can be in command of keeping the operating point of the PV array at MPP. This is done with the computational MPPT algorithm. [13]

3.2.1 PV Cell Basic Concept

The construction of PV cell is analogous to that of typical diode with PN junction. In above fig 3.2 when light emits on solar cell it is absorbed by PN Junction circuit, after that energy absorbed by the photon is supplied towards the electron-photon system of the given material, which generates the charge carrier who is split at the junction. [14] There are two forms of the charge carriers one is electron-ion pairs

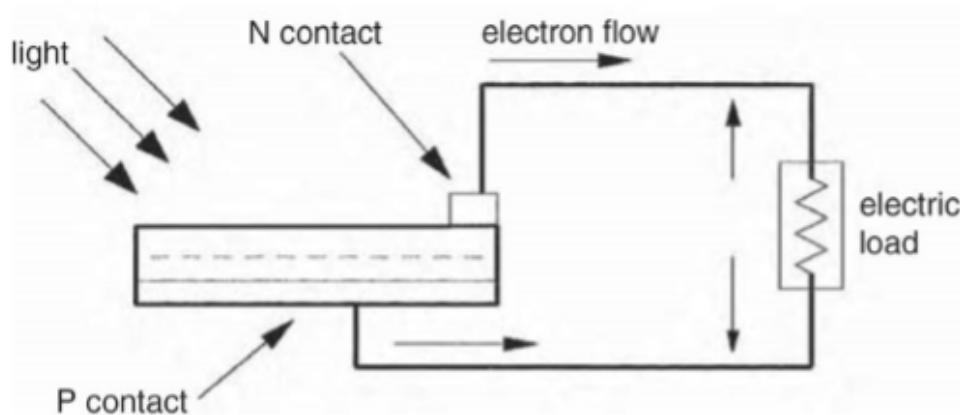


Figure 3.2: PV effect converts the photon energy into voltage across the PN junction

in the liquid electrolyte and other is electron-hole pairs at solid-semi conducting material. Charge carriers presented in the junction section make the potential gradient, also it accelerated in the electric field, and it circulated over external circuit as a current. The power which is converted into electricity is calculated by using the multiplication of square of current to the resistor. The power which remains after the conversion of electricity maintains the temperature of cell and dissipates into surrounding. [14] After comparing alternative power generation technologies, main quantity is the energy cost per Kilo-Watt Hour distributed. In case of PV power, this cost is mainly depended upon two different constraints, first is the PV energy conversion efficiency and other is the capital cost per watt capacity. Both of these constraints together will show the economic competitiveness of PV electricity. PV cell conversion efficiency is defined as follows,

$$Efficiency = \frac{ElectricalPowerOutput}{SolarPowerimpingingcell} \quad (3.1)$$

The main aim of PV cell research and development is to increase the conversion efficiency and additional performance constraints to decrease cost of commercial solar modules and cells. The other goal is to greatly enhance the manufacturing yields, although decreasing energy consumption and manufacturing cost and decreasing impurities and defects. This can be done by developing fundamental understanding of basic physics of PV cells. There are different forms of PV technologies accessible in the market in terms of conversion efficiency and the module cost because of continuous development effort to produce more efficient low-cost

cells.

3.2.2 Modeling of PV cell

The equivalent circuit of solar cell show in Fig 3.3. The characteristics equations show that the current produced by the current solar cell is equal to the current source, which flows through the diode, which flows from the shoot resistor.

$$I = I_L - I_D - I_{Sh} \quad (3.2)$$

Ideal PV Cell (Diode Equation)

Illustrates the single diode model of PV cell show in figure 3.3

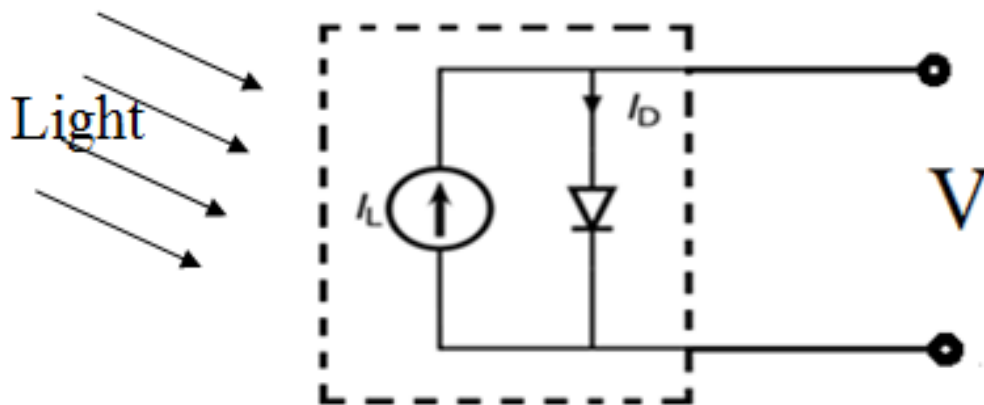


Figure 3.3: Ideal PV Cell

$$I_D = I_O * \left(\frac{q(Vd)}{e^a k T} - 1 \right) \quad (3.3)$$

I_D =Diode current in Amp

$q(Vd)$ =Chagre of elctron in coloumbs

T =Temperature in kelvine

K =Boltzman constant

a =Diode Idealy factor (1 and 2)

I_0 =Reverse saturation current in Amp

Series Resistance

$$I = I_L - I_O \left(\frac{V - IR}{e^{akT}} \right) - 1 \quad (3.4)$$

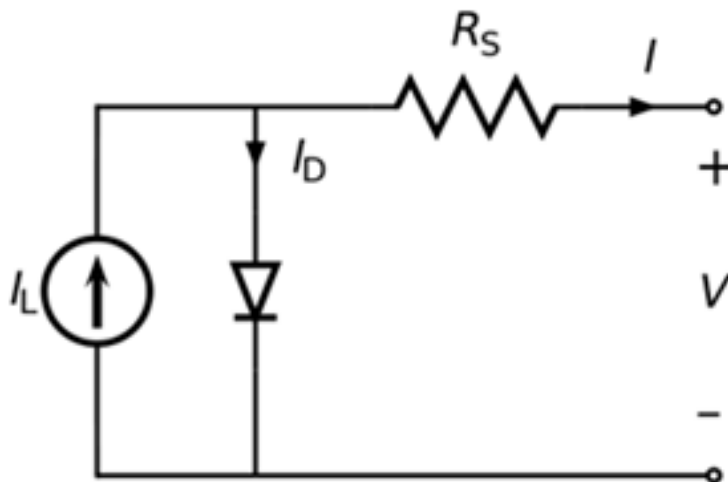


Figure 3.4: Series Resistance

Now,

$$V_j = V - IR_s \tag{3.5}$$

$$I = I_L - I_0 \left(\frac{V_j}{e^{akT}} - 1 \right) \tag{3.6}$$

Where, I_L =Photogenerated current in Amp

V =Voltage across output terminal in Volt

R_s =Series resistance in Ohm

V_j =Voltage across both diode and resistor R_s

Shunt Resistance

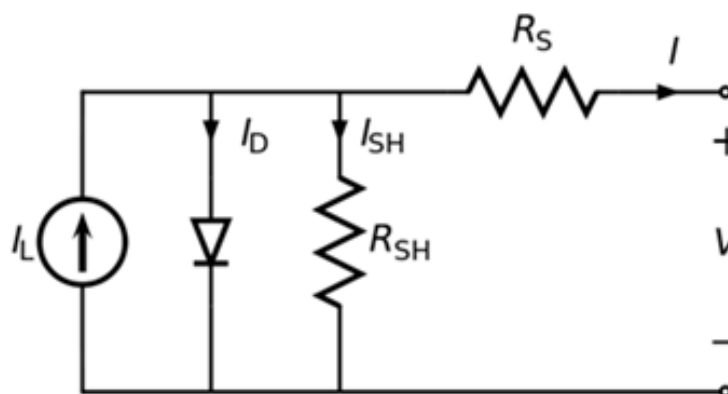


Figure 3.5: Shunt Resistance

$$I_{Rsh} = \frac{V_j}{R_{sh}} \quad (3.7)$$

Where, R_{sh} =Shunt resistance in Ohm

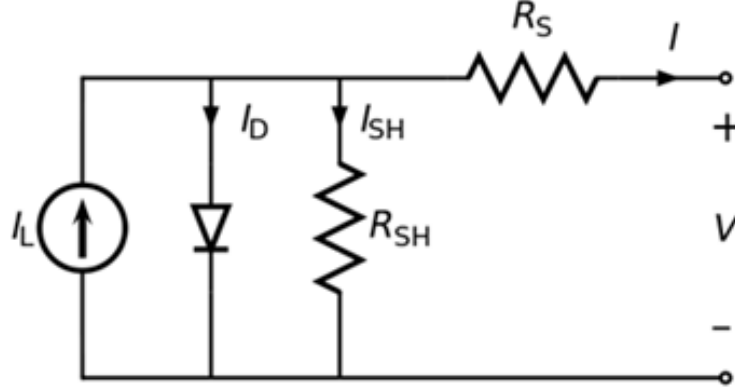


Figure 3.6: Equivalent circuit of solar cell

$$I = I_L - I_o \left(\left(\frac{V_j}{e(akT)} \right) - 1 \right) \frac{V_j}{R_{sh}} \quad (3.8)$$

The last term is ground drain current. Basically, it is negligible to compare I_L and I_D and so ignore. The saturation current of the diodes can be determined by applying the output voltage V to the cell in the dark and measuring the current in cell. This current is called reverse diode saturation current or dark current. [6]

3.2.3 I-V and P-V Characteristics

The most important electrical properties of a PV cell or a PV module are summarized in the relationship between the current and the voltage that are generated on a typical I-V characteristic of a solar cell. [15] The intensity of solar radiation (solar radiation) that hits the cell controls the current (I), while increasing the temperature of the solar cell reduces its voltage (V). Solar cells generate direct current (DC) and current voltage is equal to power so that we can create I-V curves for solar cells that represent current vs. voltage for a photovoltaic device. Characteristics of solar cells I-V Curves are a graphical representation of the operation of a solar cell or module, which summarizes the relationship between current and voltage in existing radiation and temperature conditions. The I-V curves provide the information necessary to tune the solar system so that it can work as close as possible to the maximum power point (MPP). Curve IV of a solar cell

is a superposition of curve IV of a diode of a solar cell in the dark with current generated light. Light has the effect of shifting the IV curve down into the fourth quadrant, where energy can be extracted from the diode. The backlight of the cell adds to the normal “dark” currents in the diode, so that the diode equation is ref the equation. When I-V characteristics for dark and light condition The IV curve of a solar cell is the superposition of the solar cell diode in the dark with the light-generated current as show in fig 3.7

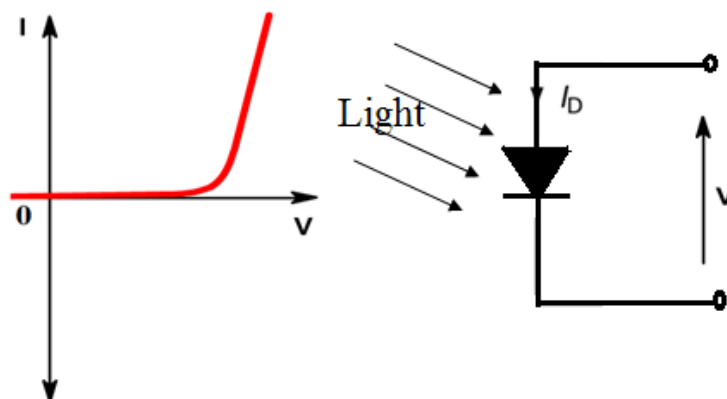


Figure 3.7: I-V characteristics for light condition

A typical voltage-to-current characteristic, known as an I / V curve, of a PN diode without a solar cell is the same with the electrical characteristics of the large diode. The applied voltage is in the direction of the feed direction. The curve shows the start and accumulation of forward bias current in the diode. When I-V characteristics for dark and light condition in main current I is flowing the circuit is equal to the negative current of $-I_D$

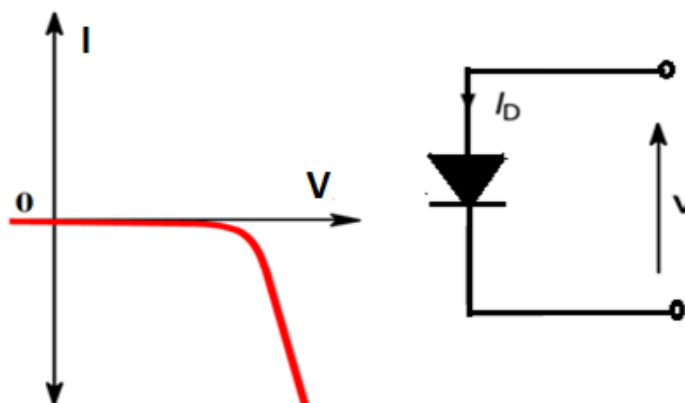


Figure 3.8: I-V characteristics for no light condition

When IV characteristics for dark and no light condition. The IV curve of the solar cell is there is no light fall in solar cell, and then the external current I is flowing the circuit. The external current is equal to the dark current I_D shown in fig. 3.8 the IV curve is shifted in negative side.

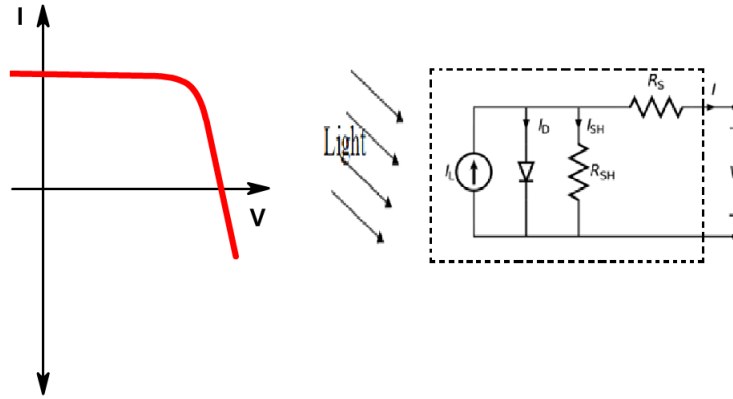


Figure 3.9: Irradiance is increase by the PV

When increase irradiance for solar cell then the current is increasing the circuit. The IV curve is shifted in the positive side as shown in fig.3.9 when irradiance in an increase in maximum limit then the IV curve is shifted in maximum current limit.

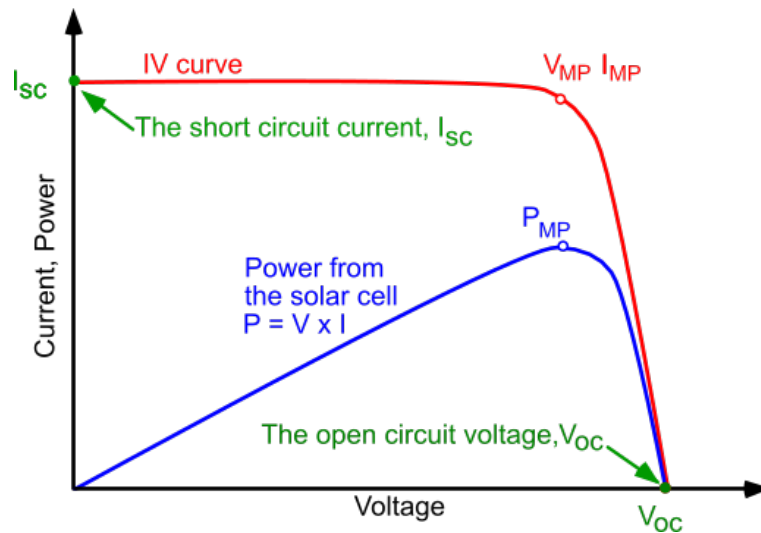


Figure 3.10: I-V curve for solar cell to get the maximum output for solar cell

The graph above shows the current-voltage characteristics (I-V) of a typical silicon photocell operating under normal conditions. The power transmitted by the solar cell is the product of current and voltage ($I \times V$). If multiplication is done, point by point, for all voltages from short circuit to open circuit conditions,

the above power curve is obtained for a given radiation level. The short circuit current as shown in fig 3.10 on Y-axis is denoted by the I_{SC} . When $I_{SC}=I_L$ then maximum possible current are flowing the PV cell because of series resistance $R_i(S)$ is very small. The I_{SC} is depend on the irradiance level. The short circuit condition in short circuit current is maximum and open circuit voltage is zero. [8] [7] The open-circuit voltage shown in fig.3.10 on X-axis it is denoted by the V_{OC} . When the maximum possible voltage from the PV cell with zero external currents. The V_{OC} is depended on the quality of the material. The maximum electrical power that a solar cell can deliver to the standard test state. If we attract the v-i characteristics of a solar cell, the maximum power will occur at the point of bending of the characteristic curve. It is shown in fig. 3.10

3.2.4 Concept MPPT

MPPT or Maximum Power Point Tracking is an algorithm included in charge controllers used under certain conditions to extract the maximum available power from the PV module. The voltage at which the PV module can produce maximum power is referred to as the "maximum power point" (or peak power voltage). The maximum power varies depending on solar radiation, ambient temperature and solar cell temperature.

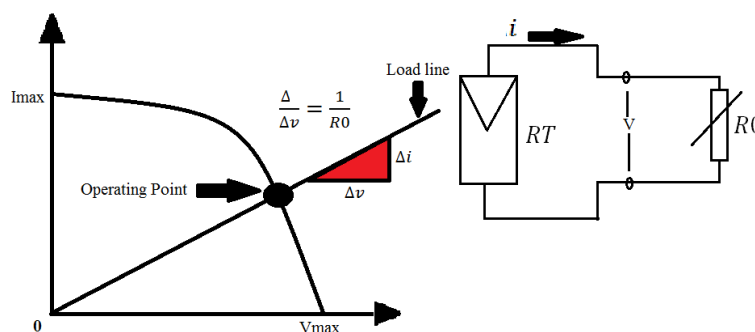


Figure 3.11: I-V curve for PV system with operating point

Think about the simple circuit as shown in Fig. 3.11. The photovoltaic model is connected with a simple resistive load R_o , R_o is capable of variable resistive load. The VI characteristics of the PV panel, which measure the voltage V and the current I of the X and Y-axis respectively. This is found near the IV loop of the PV panel. The middle line shows that the load line is in the IV line.

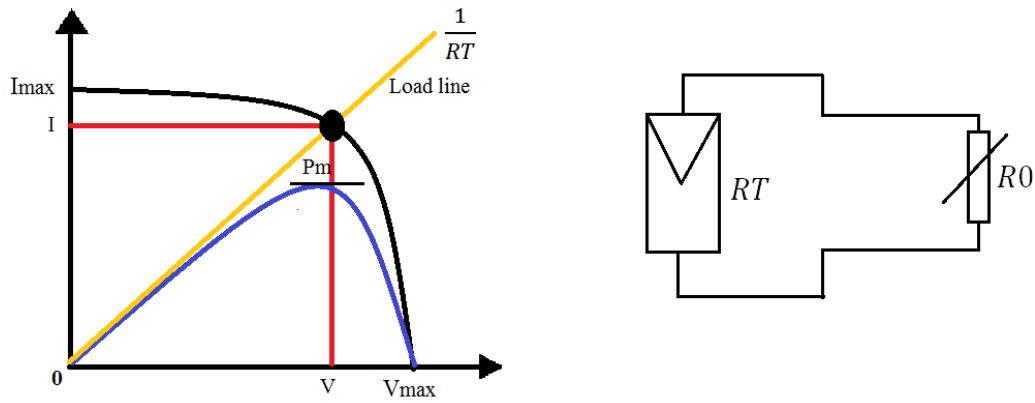


Figure 3.12: I-V and PV curves show maximum power point from PV modules

If the load line is moving along the X-axis as shown in Fig. 3.12 like $1/R_0$ the slope of line is 0 therefore R_0 to be infinite so that is open circuit across the terminal. Similarly if load line moves along the Y-axis like $1/R_0$ that is slope of the line is zero therefore R_0 is zero so that is short circuit. This operating point should represent the peak power that is being drawn. Now consider this modified figure. R_T is the resistance seen across this terminal; the terminal resistance is called R_T , R_T this is using for load line $1/R_T$.

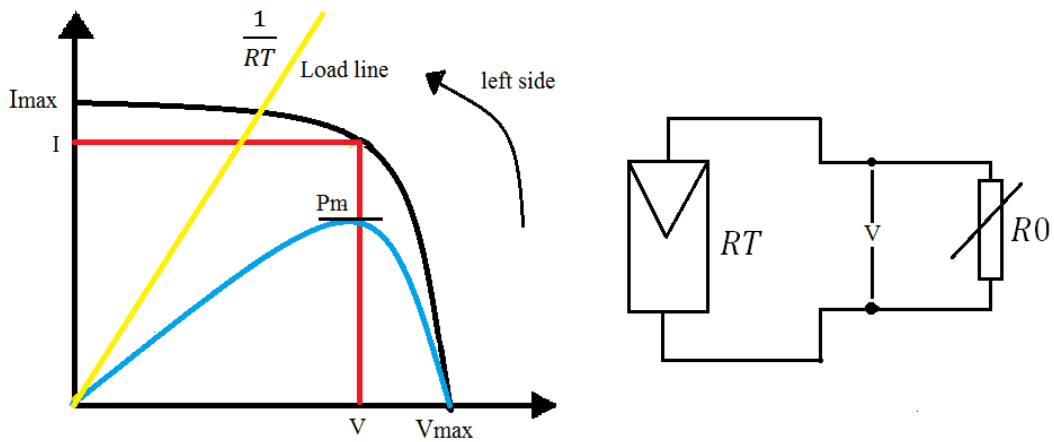


Figure 3.13: I-V and PV curves show maximum power from PV modules in load line is shifted in left side

The peak power at operating point if the line is moved to the left hand side as shown in Fig. 3.13 from operating point which represented the lowest power level, Which means that the slope has risen and the R_T has fallen, R_T means that R_0 has been fallen, it has gone up short circuited. Let me say that this operating point is tracking the maximum power point or its drawing maximum power from the PV panel. [9]

The peak power at operating point if the line is moved to the right hand side

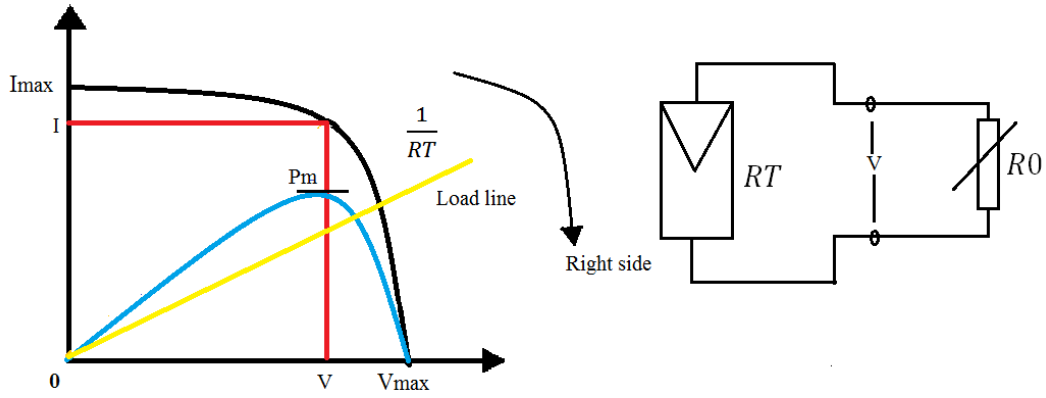


Figure 3.14: I-V and PV curves show maximum power from PV modules in load line is shifted in right side

from operating point which represented the highest power level as shown in Fig 3.14 here, which means that the slope has fallen and the R_T has risen, R_T means that R_0 has been increased, it has gone up open circuited. So this operating point does not draw the peak power from the PV panel it draws a power much less than the PV panel.

3.2.5 Mathematical modeling of MPPT (Incremental Conduction Algorithm)

In the incremental conduction method of the array terminal voltage is always adjusted according to MPP voltage is based on incremental and the instantaneous conduction of the PV module.

$$\frac{I}{V} = \frac{dI}{dV} \quad (3.9)$$

where $\frac{I}{V}$ = is instantenious conductance $\frac{dI}{dV}$ = is incremental conductance

Now, $\frac{dP}{dV} = 0$

The equation is change in power with respect to change in voltage is equal to zero.

$$\frac{dI}{dV} = \frac{d(IV)}{dV} = I \frac{dV}{dV} + V \frac{dI}{dV}$$

$$\frac{dP}{dV} = \frac{d(IV)}{dV} = I + V \frac{dI}{dV}$$

The MPPT reached when $\frac{dP}{dV} = 0$

$$0 = I + V \frac{dI}{dV}$$

That is,

$$\frac{dI}{dV} = \frac{-I}{V}$$

The slope of PV array power curve is zero at the MPP, the MPP is increase on left hand side and the MPP is decrease on right hand side. The basic equation of this method is as fallows.

$$\frac{dI}{dV} = \frac{-I}{V}$$

$$\frac{dI}{dV} = \frac{-I}{V} \text{ MPP is increase in left hand side}$$

$$\frac{dI}{dV} = \frac{-I}{V} \text{ MPP is increase in right hand side}$$

The different operating point of MPP is as follows,

$\frac{\Delta P_{pv}}{\Delta V_{pv}}=0$ then ; MPP voltage $\frac{\Delta P_{pv}}{\Delta V_{pv}}=0$ then $V_p =$ equal MPP voltage $\frac{\Delta P_{pv}}{\Delta V_{pv}}=0$ then V_p ; MPP voltage

Where I and V are the output current of the P-V array output voltage and current respectively. His left side the equations represent the incremental conduction of P-V module and right side represent instantaneous conduction. When the change report in the output conduction is equal to the negative result conductivity, solar array will work at maximum power point.

3.3 DC-DC coverter

A boost converter (step-up converter) is a DC-to-DC power converter that steps up voltage (while stepping down current) from its input (supply) to its output (load). It is a class of switched-mode power supply (SMPS) containing at least two semiconductors (a diode and a transistor) and at least one energy storage element. A capacitor, inductor, or the two in combination. To reduce voltage ripple, filters made of capacitors (sometimes in combination with inductors) are normally added to such a converter's output (load-side filter) and input (supply-side filter). [16]

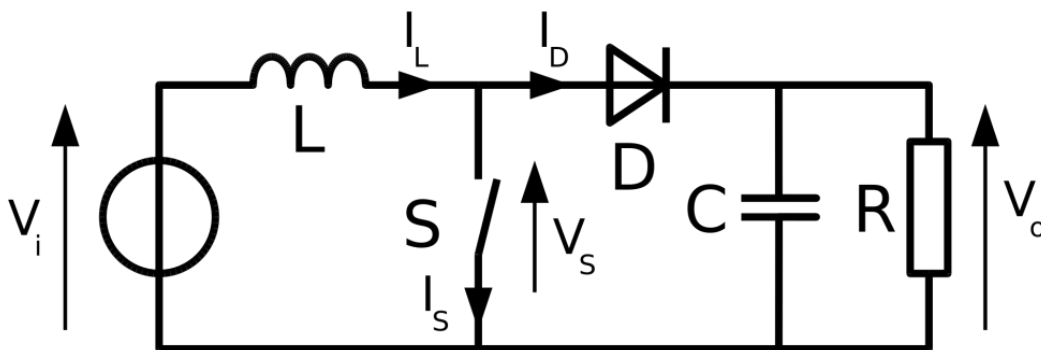


Figure 3.15: Boost Converter

The boost converter is the tendency of an inductor to resist changes in current by creating and destroying a magnetic field. In a boost converter, the output voltage is always higher than the input voltage. A schematic of a boost power stage is shown in Fig. 3.17 The basic principle of a Boost converter consists of 2 distinct states

1. Mode I- When the switch is closed, current flows through the inductor in clockwise direction and the inductor stores some energy by generating a magnetic field. Polarity of the left side of the inductor is positive.

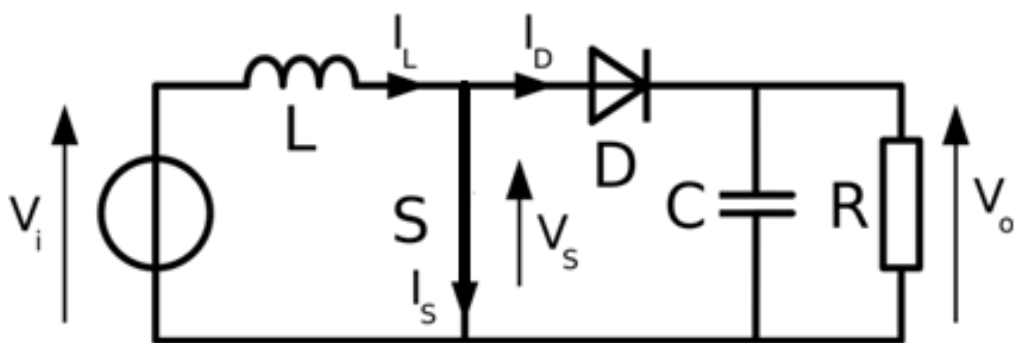


Figure 3.16: Mode I Switch is closed

2. Mode II- When the switch is opened, current will be reduced as the impedance is higher. The magnetic field previously created will be destroyed to maintain the current towards the load. Thus the polarity will be reversed (means left side of inductor will be negative now). As a result, two sources will be in series causing a higher voltage to charge the capacitor through the diode D .

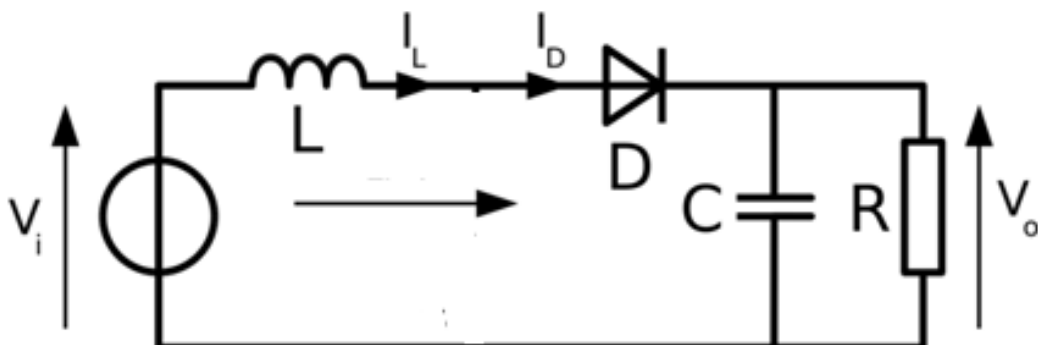


Figure 3.17: Mode II Switch is open

The voltage and current relation for the inductor L is:

$$I = \frac{1}{L} \int_0^t V dt + I_0 \quad (3.10)$$

or

$$V = L \frac{di}{dt} \quad (3.11)$$

where, I= Input current in Amp Io= Output current in Amp For rectangular pulse,

$$I = \frac{Vt}{L} + I_0 \quad (3.12)$$

when switch is closed (S=close),

$$I_i = \frac{(V_{in} - V_s) * T_{on}}{L} + I_0 \quad (3.13)$$

where, Vin= Input voltage in Volts Vs = Voltage across switch in Volts Ii = Input current in Amp Io= Output current in Amp

$$\Delta I = \frac{(V_{in} - V_s)T_{on}}{L} \quad (3.14)$$

When switch is open (S=Open)

$$I_o = I_i - \frac{(V_o - V_{in} + V_D)T_{off}}{L} \quad (3.15)$$

where, Vo= Output voltage in Volt VD= Voltage across diode in Volt

Now the equation through Delta,

$$\frac{(V_{in} - V_s)T_{on}}{L} = \frac{(V_o - V_{in} + V_D)T_{off}}{L} \quad (3.16)$$

$$(V_{in} - V_s)D = (V_o + V_D) * (1 - D) \quad (3.17)$$

$$V_o = \frac{(V_{in} - V_s)D}{1 - D} - V_D \quad (3.18)$$

Now, neglecting the voltage drop across diode and switch,

$$V_{out} = \frac{V_{in}}{1 - D} \quad (3.19)$$

So it is clear that the output voltage is directly related to the operating cycle.

The main challenge in designing a converter is the type of inductor to be used. It can be seen from the above equations that the inductance is inversely proportional to the breaking current. To reduce deflection, a larger inductor must be used. [17]
 Now, calculate the component

1. Load resistance

$$R_L = \frac{V_o}{I_o} \quad (3.20)$$

2. Duty Cycle

$$D = 1 - \frac{V_i n}{V_o} \quad (3.21)$$

3. Capacitor

$$C = \frac{I_o * D}{F_s * \Delta V} \quad (3.22)$$

where,

$$\Delta V = ESR \frac{I_o}{1 - D} + \frac{\Delta I_n e w}{2} \quad (3.23)$$

4. Inductor

$$L = \frac{V_s * D}{F_s * \Delta I_o} \quad (3.24)$$

3.4 DC-AC Inverter

An inverter is used to supply the load connected to its output socket with 220 V AC without interruption. It provides a constant AC power supply at its output jack, even if the AC power supply is not accessible. [14]

This is a combination of portable electricity, electricity and battery. The power steering stops charging the battery when the service is available and when the alternating current is turned on, the power source controls the direct current energy stored in the battery and is converted into an alternating current source of 220 V / 50 Hz, which can be used to power any conventional mechanical or computer power supply . The opposite effect occurs when the alternating current is replaced by direct current and works by disconnecting the direct current source in various ways.

To understand how a number is read, it is possible to know the number of variables that can be identified by the numbers selected by the sequence number in the order $Sw1 Sw2 Sw3 Sw4 Sw5 Sw6 Sw1 Sw2$, Finding the rotation time is 360 degrees. It can be seen that each direction is set for 180 and the rotation

angle is 60 degrees. The top and bottom of the pole are adjustable accordingly. To change the production process, the process can be disrupted.. [10]

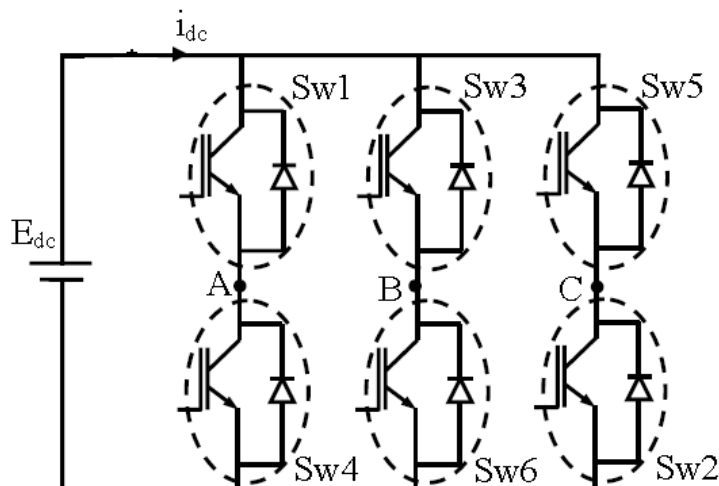


Figure 3.18: Three phase inverter

Given the balance in the switching circuit, you can find that every three cycles rotate. It can be two from the top of the switches, which is associated with a good automotive direct current, and one with a low or vice versa (that is, one from a high height and two from a low height). Six combinations for switching switches during production: - (Sw5, Sw6, Sw1), (Sw6, Sw1, Sw2), (Sw1, Sw2, Sw3), (Sw2), Sw3, Sw4), (Sw3, Sw4, Sw5), (Sw4, Sw5, Sw6). Each of the complete switches is directed at 600 in the sequence mentioned above to form a series of sets A, B, C. It will be shown later that an integral part of the three volumes will be created. have a balance. The shape of the welding adapter will be slightly different from the light switch and will work in the next section.

All three require the use of two types of fluid flow, a sine wave and a sine wave. The difficulty of this method is greatly increased with each loading option. Figure 3.19. Explores three different transport modes in a single graph [25]. The flying sine wave is required to be of any kind, but many loads can be run over the sine wave. An important aspect of the modified sine tone is the reduction of performance as well as the increase in noise and operating systems. A small (but still very large) amount of energy can fly to an environment. Due to the huge difficulties associated with designing a sine wave inverter, and the low cost that can run this square wave inverter, our team decided to go with the modified sine

wave inverter. This can be achieved by extracting the outer wave, and its filtering is like the sound of waves. The results you want will be similar to the average of the three waves.

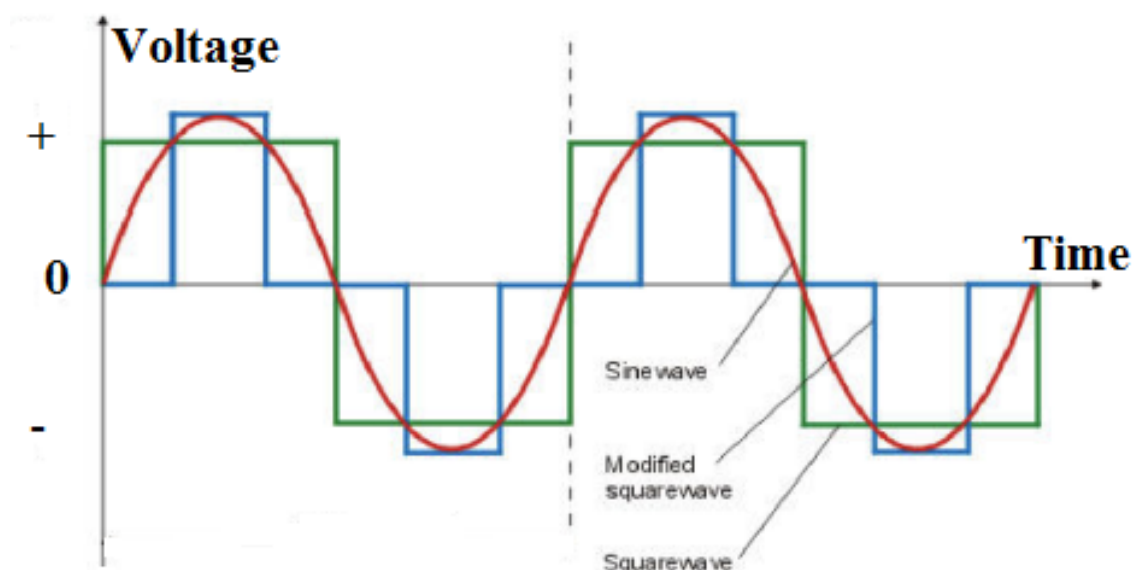


Figure 3.19: Output Wave Form of Inverter

Fig 3.19 shows the three different waveforms on a single graph. A pure sine wave is required to run any type of load, but most loads can run on a modified sine wave. The primary side effect to a modified sine wave is a decrease in efficiency and an increase in noise in the system. Fewer (but still a significant amount of) loads can run on a square waveform. Because of the immense difficulty associated with designing a pure sine wave inverter, and the limited amount of loads which can run off of a square wave inverter, our team decided to go with a modified sine wave output. This can be obtained by producing a square wave from the output, and filtering it to resemble a sine wave. The desired result would look like an average of the three waveforms presented in Fig 3.19 [18]

The vertical axis is Voltage, while the horizontal is Time. As can be seen, the red waveform is a pure sine wave, blue is a modified sine wave, and green is a square wave. The specified period would vary based on desired frequency. [11]

This is a fairly straightforward inverter that provides 220V AC when a 12V DC source is provided. It can be used to power very light loads such as night lights and cordless phones, but can be converted into a high-performance inverter by adding more MOSFETs. It uses 2 power IRFZ44 MOSFETs to drive the output

power and the 4047 IC as a stable multivibrator operating at a frequency of about 50 Hz.

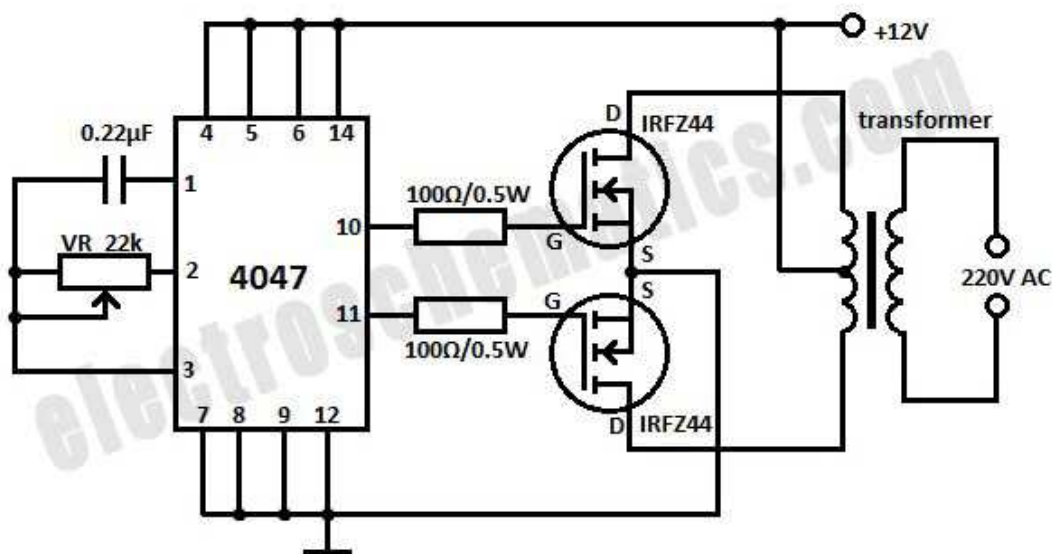


Figure 3.20: Inverter using IC CD4047

As shown in Fig. 3.20 the 10- and 11-pin outputs of the IC direct-acting MOSFETs used in a push-pull configuration. The output transformer has 12V-0-12V, 3A on the secondary and 230V on the primary. Use appropriate radios for MOSFETs.

3.5 Closure

This chapter includes a brief description, mathematical modeling of PV cell model, characteristics of PV model, concept of MPPT, and, mathematical modeling, working of DC-DC boost converter, DC-AC inverter.

Chapter 4

Methodology

4.1 Introduction

The microgrid is connected to the medium-voltage network at the point common coupling (PCC) via the circuit breakers. When the microgrid is connected to the network, the operational voltage and frequency control are entirely carried out by the network; however, the micro-grid still provide critical loads in PCC, acting as a PQ bus. In the island state, the micro-network must operate independently, independently of the network, to control the voltage and frequency of the microgrids, and therefore acts as a solar bus (supply voltage). Operation and management in both modes are controlled and coordinated using micro-source controllers at the local level and a central controller at the global level. Controlling the frequency of a traditional synchronous generator [3], controlling the frequency and voltage of a microgrid can also be performed using droop control methods [10].

In this work, it provides a rapid response to voltage and frequency control over secondary control. The analogy between inverter control and control of an insulated microgrid synchronous generator is studied [9]. In islanding mode, it is necessary to generate a reference voltage and frequency signals in the microgrid inverter control. Operating and controlling a DER inverter interface like a solar (PV) in a microgrid is a real challenge, especially if both the microgrid voltage and frequency must be kept within acceptable ranges. Voltage Control Method Based on Conventional Voltage Control for Voltage Reduction Through Voltage Control capability [18]. With V-F or P-Q control using solar PV including MPPT control and battery storage in the microgrid. In we study the frequency control

with PV in micro grades. a small-scale PV is considered to be a network-switched mode for controlling the active and reactive power of the system. Here, the control methods consider the abc-dq0 transformation and vice versa, which is avoided in this document [21]. In there are a number of control algorithms through which PV generators are capable of controlling voltage and frequency (V-f) and controlling active and inactive / reactive power (P-Q) in insulated and grid-connected microfibers. MPPT control on PV side, battery control and V-F / P-Q control algorithm on inverter side. These three control algorithms are connected in three stages together via a power balance on the DC and AC sides of the inverter so that the DC side voltage is indirectly controlled to the desired value [21].

4.2 V-F and P-Q Control Strategy

In the proposed network of this paper, all the DGs are assumed to be inverter-interfaced. Also switching transients, harmonics and inverter losses are negligible. Since in a flexible MG, the power regulation of each DGs should be not only determined by the load demand, but also controlled based on the power available in RES unit, we have presented two control strategies for island operation of a MG in this section. VF control aims at controlling active and reactive power and also frequency and voltage regulation. On the other hand, PQ control aims at adjusting active and reactive power of RES at MPPT reference point.

4.2.1 PQ control mode

So far, much research has been done on the advanced control strategies of RES in PQ mode [19]. In an islanded MG, however, there is a limitation of power generation for the RES unit. Because of these special situations, the entire system must operate in a flexible manner with coordinated power control between RES and other DGs operating under VF control. As already mentioned, RES in the PQ control mode provides constant active and reactive power to the MG based on the MPPT strategy. These control strategies were used and implemented based on the dq0 reference frame transformation, which determines the d and q axis components of the AC side streams. [13] Modeling assumes that the network model and loads are represented in the coordinate system of one of the individual VSIs. This reference system is considered a common reference system. All other VSI will be

transferred to this common coordinate system. PLL is used to synchronize RES with MG. In addition, the frequency of this device is determined by DGs operating under VF control to achieve this disconnected control. The controller contains two loops. The first is the power control loop, and the second is the current control loop. The power control loop determines the current settings. The current component along the d axis is used to control active power, and the component along the q axis to control reactive power by setting the d axis in accordance with the mains voltage [8]. Thus, the setting of the current component along the d axis is fixed by the active power control loop, and the current component along the q axis is fixed by the reactive power control loop.

Active power and reactive power transmitted to the AC system by RES are calculated in accordance with (1) and (2).

$$P = \frac{3}{2} * [V_{pccd} * i_d + V_{pccq} * i_q] \quad (4.1)$$

$$Q = \frac{3}{2} * [-V_{pccd} * i_q + V_{pccq} * i_d] \quad (4.2)$$

where V_{pccd} and V_{pccq} are the AC system dq frame voltage components and cannot be controlled by the VSI system.

$$P = \frac{3}{2} * V_{pccd} * i_d \quad (4.3)$$

$$Q = \frac{3}{2} * -V_{pccd} * i_q \quad (4.4)$$

so P and Q delivered can be controlled bt i_d and i_q respectively

$$i_{dref} = \frac{2}{3 * V_{pccd}} P^* \quad (4.5)$$

$$i_{qref} = \frac{2}{3 * V_{pccd}} Q^* \quad (4.6)$$

so i_{dq} follows i_{dqref} properly if the control system can provide fast reference tracking. Also P and Q can be independtly controlled by their respective reference commands P^* and Q^* which are the outputs of MPPT controller. The current control loop has been considered as conventional proportional-integral (PI) controller which is represented in Fig.4.1. The output of the Current controller is

given to the inverter as the demanded voltage for switching. [19]

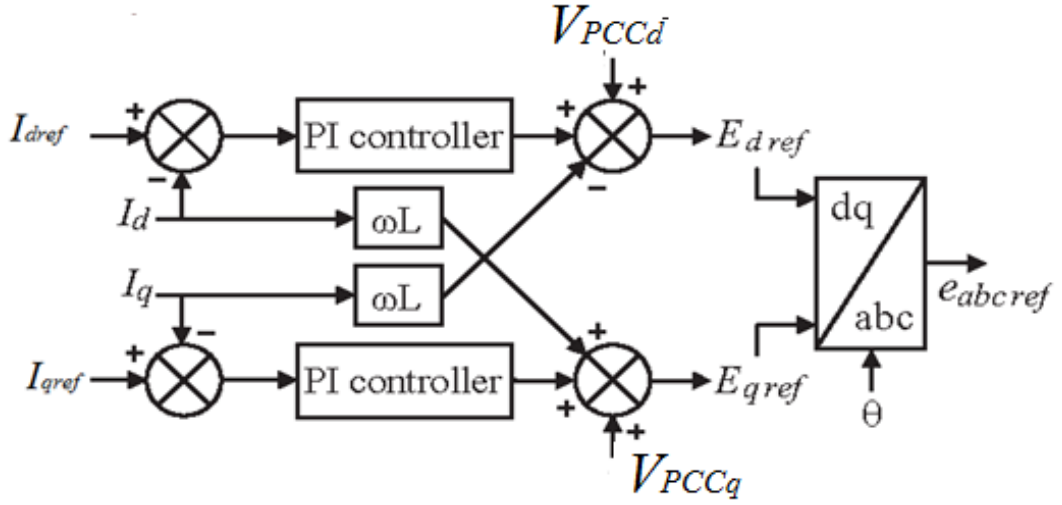


Figure 4.1: Inner current control loop

4.2.2 VF control mode

Regulation of voltage and frequency in an autonomous MG will be performed by the DGs operated under VF control (VFDGs). In this case, at least one VSI should be operated in VF control mode to regulate the system voltage and frequency within the acceptable limits [9]. The excellence of this control strategy is that no communication infrastructure is needed, thereby using only local measurements for the MG control in a decentralized method, and plug-and-play operation. The block diagram of the VSI used VF is shown in Fig.4.2 For these units, we will adopt the traditional soil management plan. The control of VF-DGs consists of three components, the condenser, the power supply and the current controller. The detector detects the magnitude and timing of the output voltage according to the compression characteristics and capacitance and power output. The power supply and drive are designed to withstand normal pressures and provide value for the output voltage of a VSI. The operating forces and electrical conductivity of the dq frame are calculated by measuring the output current and output voltage as follows.

$$P = \frac{3}{2} [V_{pccd} * i_d + V_{pccq} * i_q] \quad (4.7)$$

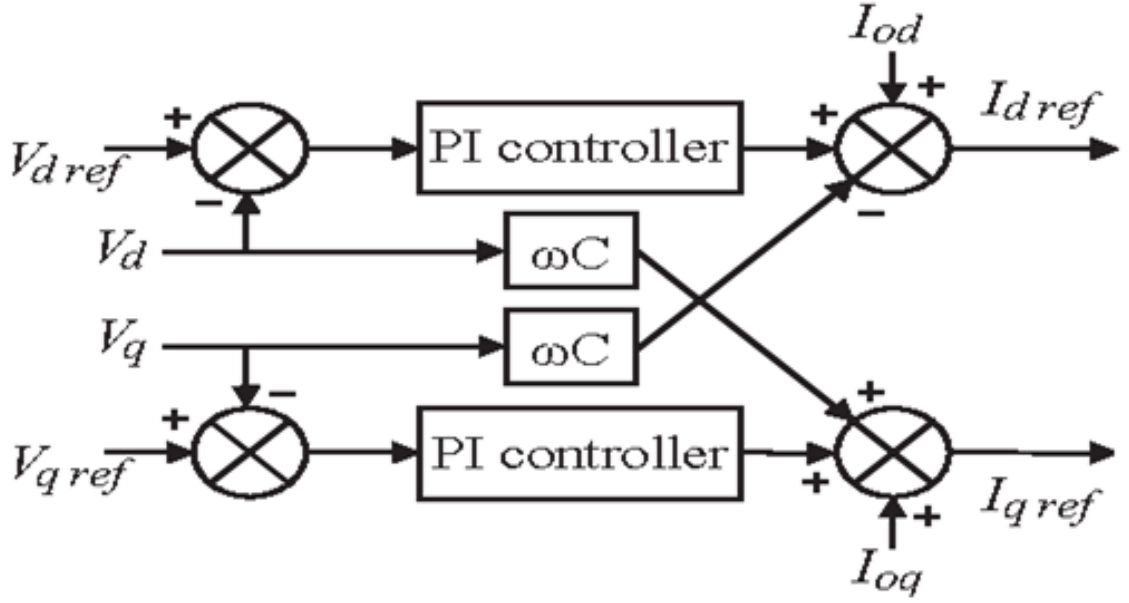


Figure 4.2: outer voltage loop

$$Q = \frac{3}{2} * [-V_{pccd} * i_q + V_{pccq} * i_d] \quad (4.8)$$

The active reactive power share between Voltage and frequency distribution grid based on drop gain as in equation (9) and (10).

$$w_{ref} = w_{pcc} - m_p P \quad (4.9)$$

$$V_{ref}^* = V_{pcc} - n_q Q \quad (4.10)$$

Where w and v^* denote the frequency and voltage of inverters, and w_n and v_n are their respective values. Also p_m and q_n are the sum of the coefficients. Depending on the type of DG, the coefficients can vary and are calculated using (11) and (12) for transmission.

$$m_p = \frac{w_{pccmax} - w_{pccmin}}{P_{max}} \quad (4.11)$$

$$n_q = \frac{V_{ref}^* - V_{pcc}}{Q_{max}} \quad (4.12)$$

4.3 Control loops

Inner current control loop

The inner current loop in a small signal can be done on equation (13) to obtain small signal transfer function. The separation of real part and imaginary part aligns the d axis along with V_{PCC} ($V_qPCC = 0$) now the rewrite the equation of d-q axis as follows.

$$V_{dref} = L_1 \frac{di_d}{dt} - w_{pcc} L_l i_q + R I_l * i_d + V_{dpcc} \quad (4.13)$$

$$V_{qref} = L_1 \frac{di_q}{dt} - w_{pcc} L_l i_d + R I_l * i_d \quad (4.14)$$

Neglecting the stitching terms in (13) and think about it only small parts of the signal can we get a small signal Deviations according to (14). The equation (13) is transform to matrix form give as.

Small signal control current transfer functions for the inner loop can easily be written as

$$G_{id} = \frac{i_d(S)}{V_{dref}(S)} = \frac{1}{(sL + R)} \quad (4.15)$$

$$G_{iq} = \frac{i_q(S)}{V_{qref}(S)} = \frac{1}{(sL + R)} \quad (4.16)$$

The control functions in the current distribution are simple in first order systems whose pole depends on line inductance and resistance. So, Proportional integral it can be designed for the inner current loop taking into account the line values. Because the flow through the line is controlled, the only inductor for switching components necessary accords to base on this, the value of inductance is given.

Outer Voltage loop

In standalone(Autonomous) mode, the outer loops are configured. The outer loops of the system are the voltage loop and the acceleration loop. They can be defined

as equation(17)

$$G_v(S) = \frac{V_{dpcc}(S)}{V_{dref}(S)} \quad (4.17)$$

Transfer function can be obtained taking into account the dynamic equation for RLC load in the autonomous mode.

$$\frac{d_i s}{dt} = \frac{V_{pcc}}{L_{load}} + C_{load} \frac{d^2 * V_{pcc}}{dt} + \frac{1}{R_{load}} * \frac{dV_{pcc}}{dt} \quad (4.18)$$

$$L_{load} \frac{d}{dt} = (V_{dpcc} - V_{pcc}) e^{-j\omega pcc t} + L_{load} C_{load} \frac{d^2}{dt^2} [(V_{dpcc} - V_{qpcc}) e^{j\omega pcc t}] + \frac{L_{load}}{R_{load}} \frac{d}{dt} [(V_{dpcc} - V_{qpcc}) e^{j\omega pcc t}] \quad (4.19)$$

Consider the operating point V_{ref} , $i_{d,wref}$ and i_q . A small signal deviation from this steady operating point can be considered like the case before. The cross coupling are neglecting and V_qPCC is assumed to be zero.

$$G_v(S) = \frac{V_{dpcc}(S)}{V_{dref}(S)} = \frac{R_{load}}{sL + R} \quad (4.20)$$

The next step is to get the transfer function $G_w(S)$ in equation (21)

$$G_w(S) = \frac{w_{pcc}(S)}{V_{qref}(S)} \quad (4.21)$$

In this case assumption that $V_{pCC} = V_{ref}$, $V_qPCC = 0$ and cross coupling are neglected. Under this assumption, if small signal variation in w_{pCC} and i_q are considered the equation (19) and equivalently represent the below equation (22)

$$G_w(S) = \frac{w_{pcc}(S)}{V_{qref}(S)} = \frac{1}{C_{load} V_{ref}} \quad (4.22)$$

The controller for the outer loop can be designed considering this block diagram shown in fig. 4.2. An integrator is required in this compensator also for saturating the outer loop in case of a grid connected mode. Therefore a PI with a lower cut off frequency can considered for the controller for the acceleration loop also. [20]

4.4 Mathematical Modeling

4.4.1 The Complete Control Structure of V(Q) and F(P) Strategy

In this section Equivalent Circuit for Emulating the Control Using Voltage Controlled Source the voltage source inverter as shown in fig. 4.3. The switch S1 is also used for isolator controlled purpose by connecting and disconnecting grid utility from the desired system. The status of switch S1 unknown condition from VSI, that is VSI should be the detect the change of switch S1 without knowing the status of switch S1. [21]

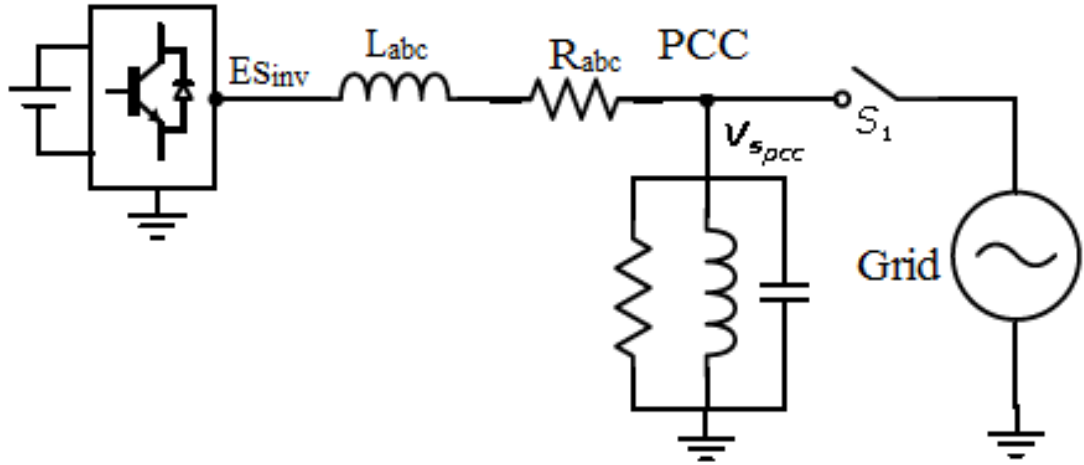


Figure 4.3: Equivalent Circuit For Emulating The Control Using Voltage Controlled Source

The control variables magnitude V and angle δ for real and imaginary power one has to deduce the control variables in the d-q frame. You have to look the performance equations in a d-q-frame. Remember that Circuit in Fig 4.2 in which S1 is open and the VSI the power to the load. The voltage control for source in equation (24) is represented by the circuit is shown in fig 4.3

$$V_{inv} = L \frac{di_s}{dt} + i_s R + V_{pcc} \quad (4.23)$$

Where, V_{inv} =Inverter voltage i_s =PCC current L =series inductance of transmission line R =Series resistance of transmission line The losses are neglected and the load demand is equal to the power supplied by the source. The power at PCC in the term of d-q axis component. The PCC voltage V_{pcc} and PCC current i_s

with respect to rotating stationery frame; this is represented by with d-q rotating frame and angular speed $w(pcc)$. as given below.

$$i_s = (i_d - ji_q)e^{(-jwpcct)} \quad (4.24)$$

$$V_{pcc} = (V_{dpcc} - V_{qpcc})e^{(-jwpcct)} \quad (4.25)$$

$$f_d + jf_q = f_s e^{(-jwpcct)} \quad (4.26)$$

Here, f_s = stationery frame f_d is d axis component and f_q q axis component of stationery frame. The angular rotating speed is w_{pcc} , The power equation at w_{pcc} is given by equation (27)

$$P_{load} = \frac{3}{2}(V_{pcc} * i_s^*) \quad (4.27)$$

$$Q_{load} = \frac{3}{2}(V_{pcc} * i_s^*) \quad (4.28)$$

The real and imaginary part is separated and making V_qPCC is made equal to zero. The power equation is given by equation (29)

$$P_{load} = \frac{3}{2}(V_{pcc} * i_{dpcc}) \quad (4.29)$$

$$Q_{load} = \frac{3}{2}(V_{pcc} * i_{qpcc}) \quad (4.30)$$

The real power and imaginary power is decoupled from the transformation to d-q frame along V_{pcc} . The PCC at real power and imaginary power is reflected by deviation in magnitude of V and relative acceleration δ with respect to v_{ref} is continuously applied by PCC. The algebraic difference between reference voltage V_{ref} and deviation in magnitude V_dPCC instantaneously is referred by the d-q rotating frame; now similarly, the algebraic difference between relative acceleration of reference space vector w_{ref} and PCC w_{pcc} The PCC of real demand is algebraic difference between $V_{dref}-V_dPCC$ from equation (29) and imaginary power demand is algebraic difference between $w_{ref}-w_{pcc}$. This imaginary power demand can be corrected by altering i_q , the control variable i_dPCC and i_qPCC) is directly

available on voltage control source. The separation of real part and imaginary part aligns the d axis along with V_{PCC} ($V_q = 0$) now the represent the dynamic equation of d-q axis as follows. [22]

The equation (30) is steady state and neglect the cross coupling term. The change in $i_d PCC$ is done by changing $V_d ref$ and the change in $i_q PCC$ is done by changing in $V_q ref$. The inner control loop variables are i_d and i_q . The i_d and i_q reference is generated in algebraic difference between $V_d ref - V_d$ and $w_r ef - w_p cc$ respectively. The controlling of line inductor L_{abc} is current controlled by the inner current control loop. The line inductor L_{abc} eliminates the low frequency and filters out the high frequency. The complete control structure is shown in fig 4.4 [23]

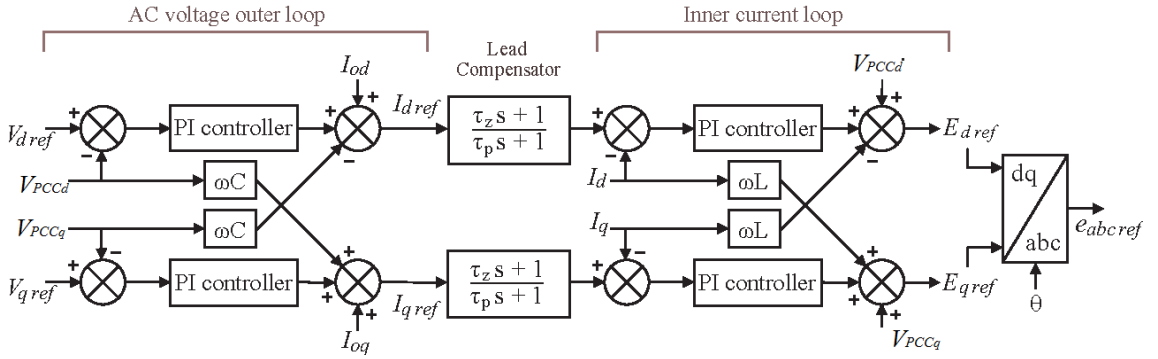


Figure 4.4: The Complete Control Structure

The voltage V_{PCC} and angular speed w_{pcc} is fixed by the grid in grid connected mode. If there is uncontrollable deviation in outer loop, then it will saturate continuously. The outer loop is transfer the inner current loop because of uncontrollable deviation is continuously saturate condition. The saturation limit i_{dmax} and i_{qmax} would be determined by the maximum power that can be taken or reduce. The i_{dmax} can be from an MPPT in this case voltage source inverter is operated as source in grid connected mode; as grid is failure V_{PCC} is maximum and therefore $V_{ref} - V_{PCC}$ is negative and the PI controller output is decrease from the outer loop is referred by the i_{dmax} . The i_{dmax} goes to lower value of power demand, and inner current loop is decrease immediately, now similar to that the grids connected mode in voltage source converter is supplying the i_{dmax} case grid is failure, w_{pcc} is increase or maximum and $V_q PCC$ is maximum by the PLL. The PI controller output is minimum or decrease, therefore $w_{ref} - w_{pcc}$ is negative,

the output of outer loop is given by the PI controller is decrease or minimum. The current i_d^{max} is come from current reference in equation (20) in comes to lower value of power demand. The PCC space vector V_{PCC} or $w_{(pcc)}$ with respect to reference space vector V_{ref} or w_{ref} is applied to direction of PCC this is correct deviation is given by the basis of control concept. [13] This concept translates the d-q rotating frame into a simple and robust implementation. When the Power ON mode is enabled in the control strategy, the inner control loop is enabled. If the autonomous mode in the control strategy function is variable in the voltage and frequency control, this control strategy depends on the state of the switch S1as shown in fig.3.14. If the switch is open in the control strategy, the voltage and frequency control loop are activated, and the switch is closed the control strategy for the inner current loop is active. The voltage controlled converter is used in local isolator switch. The current control to voltage control is use to mode detection mechanism.[14]

4.5 Mode of Operation

When the switch is open, the converter is working as a source with reference rotating frame to angular speed w_{ref} is also known as an autonomous mode. When the switch is closed, the converter is source observer or sunk of grid space vector to working d-q frame is also known as grid-connected mode shown in fig.4.3. The grid-connected mode in grid space vector is aligned the PLL and the result will the huge amount of current circulates between converter and grid by line impedance. This problem is being reduced by using the synchronization process. Synchronization process reduces the problem above. The synchronization isolator switch is checked on both side voltages and it will close the Isolator switch before the local Isolator switch is controlled by the converter that uses the synchronizing process. In case of autonomous mode. The converter is managed by the general isolator switch and it communicates with other converters. This literature has an alternative to the proposed control structure [19]. The converter generates the trigger and as a result, the system exceeds the state power limit. As soon as the PLL error sets in a limit value, the converter is switched back to a connected network. PLL Reboot will be fast enough to be fast enough. Using virtual impedance limited to current over time of conversion. That even with this method, the inverter is de-energized

until the PLL is integrated. The PCC is defect the distortion is available in grid such voltage and frequency is injected by the other signal. A small period of time converter is turn off to maintain the current limit. This control strategy issue is based on grid reference value [10].

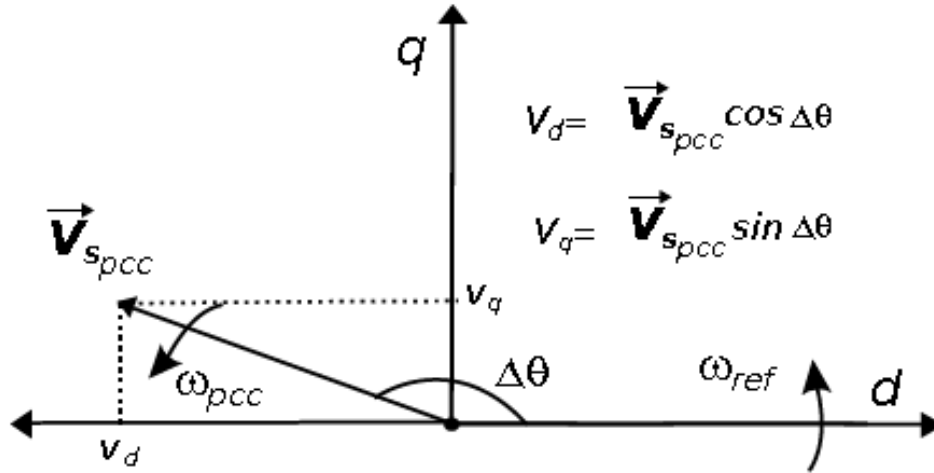


Figure 4.5: Position of Grid At Instant Transfer From Autonomous Mode To Grid Connected Mode

To make the proposed control strategy an autonomous controlling the true sense and overcome the above limitation. The synchronizations technique is a simple of PLL delay is corporate along with this control strategy [21].

4.6 Closure

This chapter includes a brief description of control strategy, and designing mathematical modeling of PQ and VF control strategy. This chapter includes the different control modes by above using control strategy.

Chapter 5

Results and Discussion

5.1 Introduction

In this chapter, the proposed system is implemented in MATLAB Simulink and simulation results are presented. Also, the proposed V-F and P-Q control strategy. The experimental results are presented in section. The MATLAB Simulink results and experimental results are then compared with each other.

5.2 Simulation and results

The PV system simulation is shown in fig. 5.1 The PV array, boost converter, inverter and injection transformer, equipped with P(F)-Q(V) controllers from nominal value inject and sunk active and reactive power for grid support purpose. The performance of the grid support V-F control strategy. The converters are a response to frequency deviation and voltage magnitude with unity power factor. The frequency and voltage below from the nominal value, the converter is operated t with increase active power in order to support the grid under low-frequency operation, and the grid voltage magnitude reduces the combined P(F)-Q(V) control strategy. The DC bus derived from photovoltaic system and maximum saturation limit. The Maximum Power Point Tracking (MPPT) is controlled the PV system and its depend on the mode of PCC. The PV cell in output voltage when the maximum possible voltage from PV cell with in external current is zero, and the output voltage is maximum in 62,5 volt and minimum in 60 volts as shown in fig.

5.2

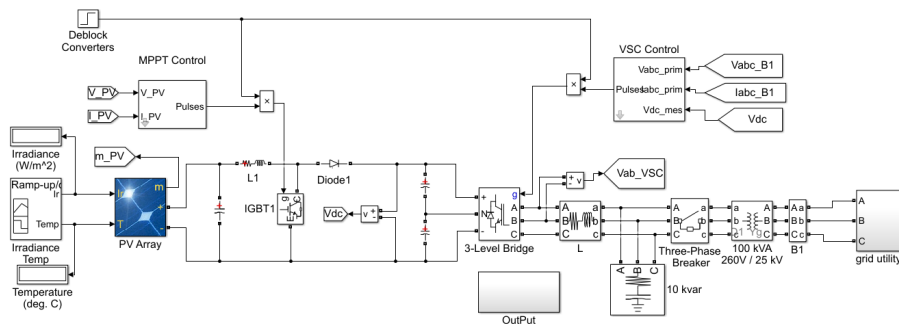


Figure 5.1: Simulation Model of PV System In Autonomous Operation

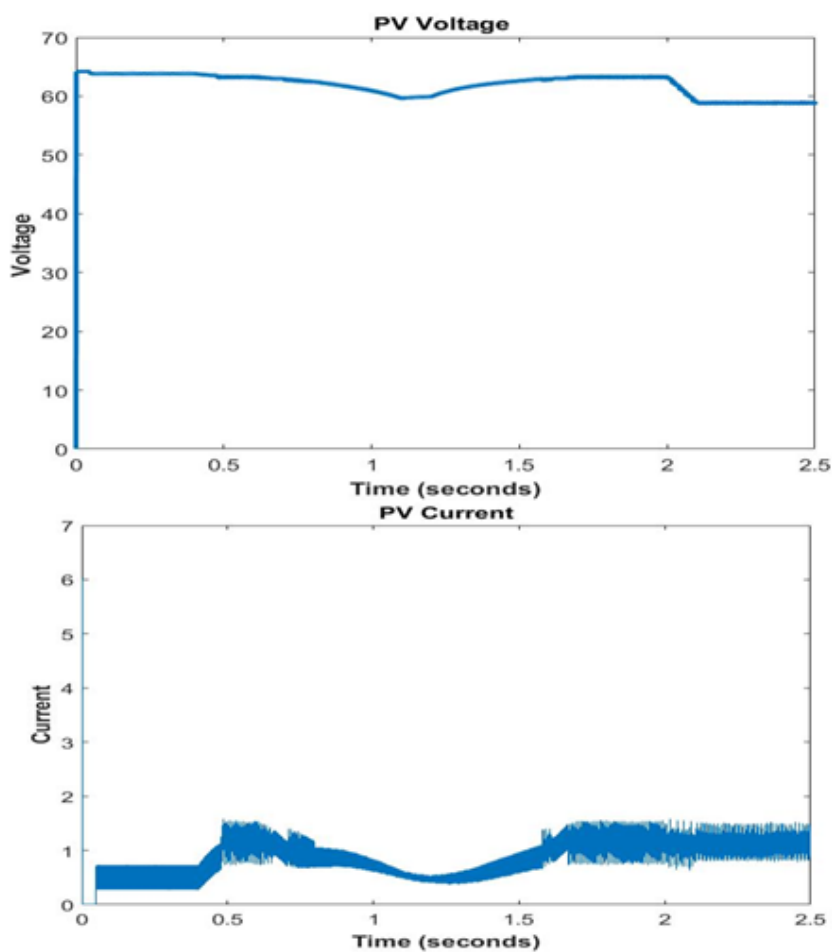


Figure 5.2: PV Voltage and Current

The simulation result as for boost converter as shown in fig. 5.3. The boost converter gives an input from PV side. The boost converter is step up the voltage and step down the current. The boost converter step up the voltage from 62 volt to 200 volts.

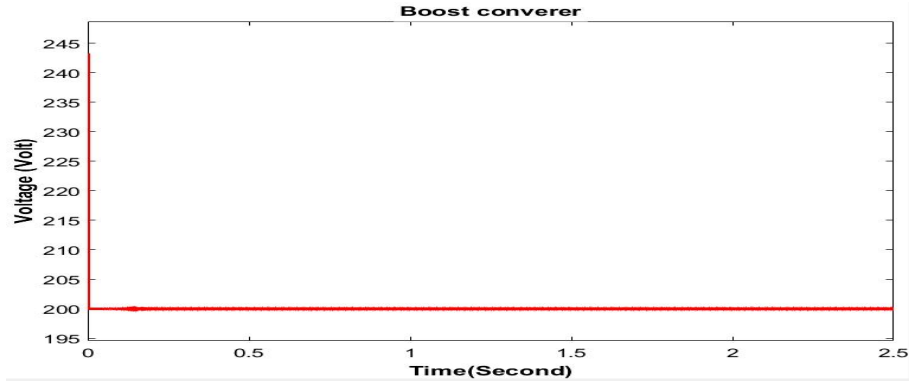
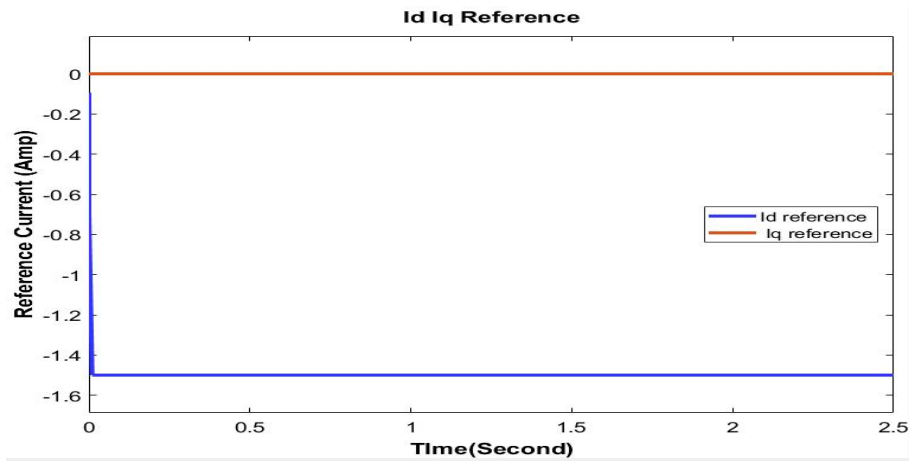


Figure 5.3: Boost converter output

The control strategy is implemented based on dq0 frame transformation that determines the d-axis and q-axis components of the ac side current. The $i_q = 0$ as shown in fig. 5.4. The P and Q delivered can be controlled by i_d and i_q for PCC and i_d and i_q reference properly. If the control system can provide fast reference tracking, also P and Q can be independently controlled.

Figure 5.4: Simulation Waveform For i_d i_q ref For Control Strategy

The real and imaginary parts are separated, and making $V_q PCC$ is made equal to zero. The real power and imaginary power are decoupled from the transformation to the d-q frame along i_q , which varies depending on the $V_q PCC$. The inner control loop variables are i_d and i_q . The i_d and i_q reference is generated in algebraic difference between i_d and i_q , but $i_q = 0$, as shown in fig. 5.5. The converter transfers the autonomous mode within 2ms because of a failure condition of the grid. Now the d-q axis current also changes because of load requirement, as shown in fig. 5.4 and fig. 5.5. The reference magnitude and speed are changed by the change in i_d and i_q because of a non-linear load. The grid-connected mode is converter function is

controlled by the maximum current limit

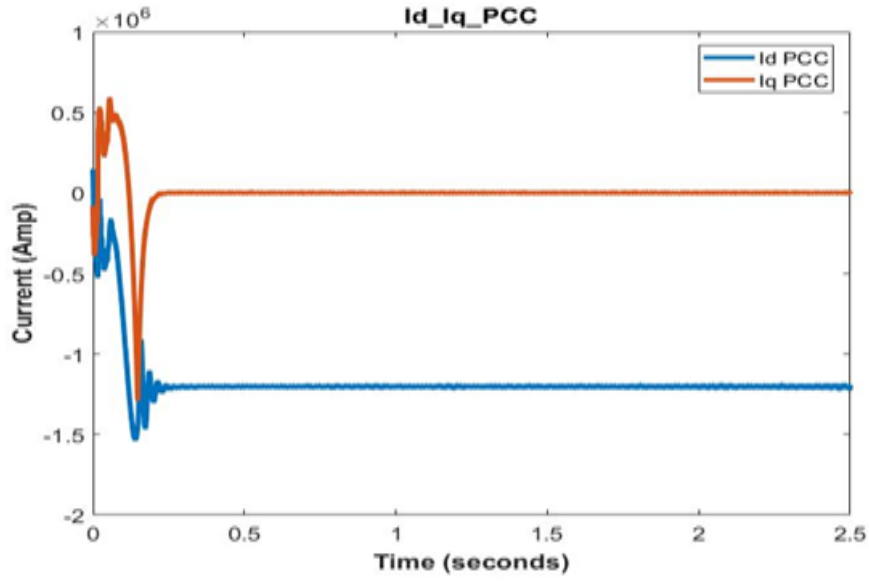


Figure 5.5: Simulation Waveform For i_d i_q PCC For Control Strategy

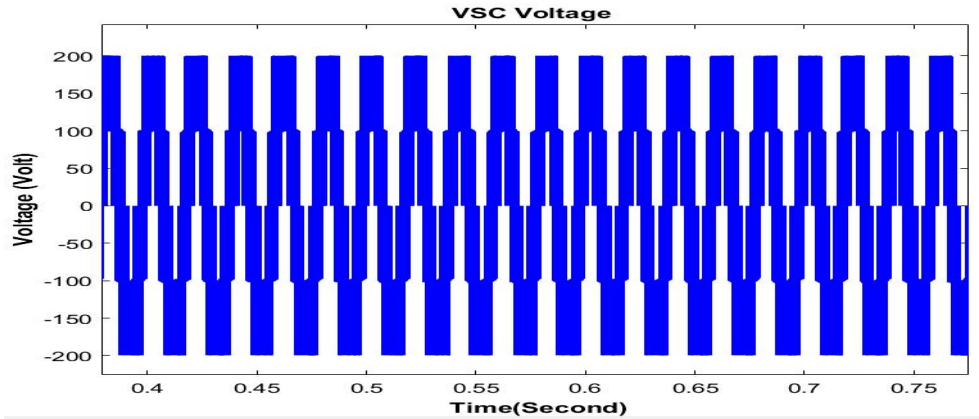
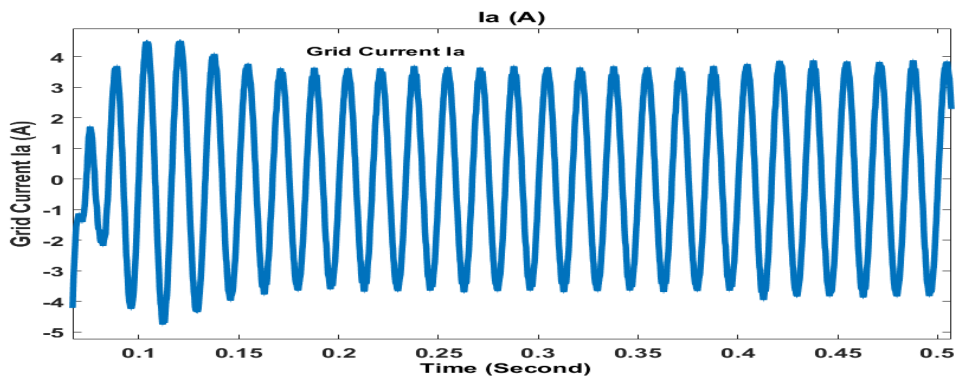
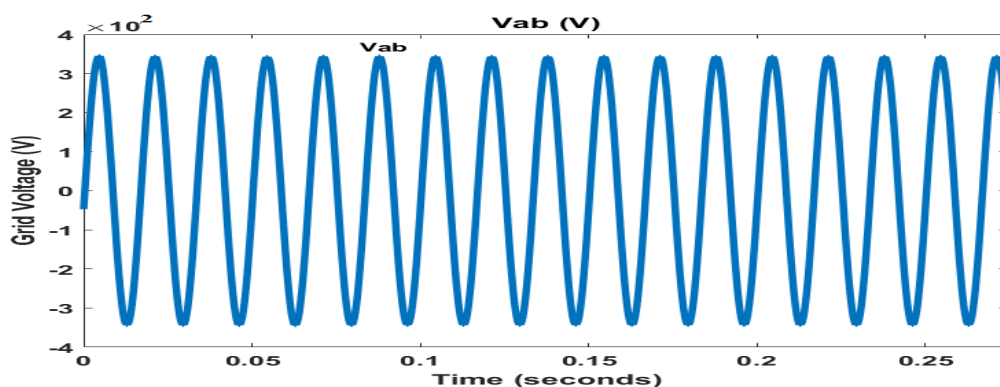


Figure 5.6: Simulation Waveform Inverter

The simulation results in its shown in fig.5.7 Waveform often grid-connected mode in proposed control strategy is depending on PCC voltage V_{ab} and grid current I_{ab} , these results in $V_{ref} > V_d$ and $w_{ref} < w_{pcc}$ it is grid connection mode operation. The waveform of autonomous mode in the proposed control strategy in $V_{ref} < V_d$ and $w_{ref} > w_{pcc}$ the transfer condition for a resistive load.

Figure 5.7: Autonomous mode grid voltage V_{ab} and grid current I_a Figure 5.8: Autonomous mode grid voltage V_{ab} and grid current I_a

In the simulation waveform is shown in fig.5.8 and 5.7. The converter easily switches to autonomous mode within 2.5 ms. To the with an RC load, the q-axis current changes to a positive value and as expected, for RL load to a negative value. In case of non-linear load the instantaneous values of i_d and i_q change to control the reference magnitude and speed. It can be unique seen that the converter works like a current-controlled Provision of the maximum current limit in the connected network Mode. In the event of a power failure, the inverter controls immediately changes the voltage frequency control to the magnitude and frequency of the PCC voltage.

5.3 Hardware and results

5.3.1 Hardware setup

The following subsection gives the information about component of proposed experimental setup.

PV module

If photovoltaic solar panels are made up of individual photovoltaic cells connected together, then the Solar Photovoltaic Array, also known simply as a Solar Array is a system made up of a group of solar panels connected together. A photovoltaic array is therefore multiple solar panels electrically wired together to form a much larger PV installation (PV system) called an array, and in general the larger the total surface area of the array, the more solar electricity it will produce. The solar module as shown in Fig 5.9



Figure 5.9: PV Module

A complete photovoltaic system uses a photovoltaic array as the main source for the generation of the electrical power supply. The amount of solar power produced by a single photovoltaic panel or module is not enough for general use. Most manufactures produce standard PV panels with an output voltage of 12V or 24V. By connecting many single PV panels in series (for a higher voltage requirement) and in parallel (for a higher current requirement) the PV array will produce the

desired power output.

Photovoltaic cells and panels convert the solar energy into direct-current (DC) electricity. The connection of the solar panels in a single photovoltaic array is same as that of the PV cells in a single panel. The panels in an array can be electrically connected together in a series, a parallel, or a mixture of the two, but generally a series connection is chosen to give an increased output voltage. For example, when two solar panels are wired together in series, their voltage is doubled while the current remains the same.

The size of a photovoltaic array can consist of a few individual PV modules or panels connected together in an urban environment and mounted on a rooftop, or may consist of many hundreds of PV panels interconnected together in a field to supply power for a whole town or neighborhood. The flexibility of the modular photovoltaic array (PV system) allows designers to create solar power systems that can meet a wide variety of electrical needs, no matter how large or small.

It is important to note that photovoltaic panels or modules from different manufacturers should not be mixed together in a single array, even if their power, voltage or current outputs are nominally similar. This is because differences in the I-V characteristic curves of the panels as well as their spectral response are likely to cause extra mismatch losses in the array reducing its efficiency.

SMPS Transformer

Switch mode power supply (SMPS) transformers are commonly used in a regulated power supply and function to step up or step down voltage or current, and/or provide isolation between the input and output side of a power supply. On the primary side of a switch mode transformer, the duty cycle (on-time) of the input voltage waveform is varied (switched) to deliver a constant output voltage under varying load conditions. SMPS transformers are designed to operate at a specific frequency, typically between 10 kHz to 500 kHz. SMPS transformer power levels now extend into the 50 kW range. [5.9](#)

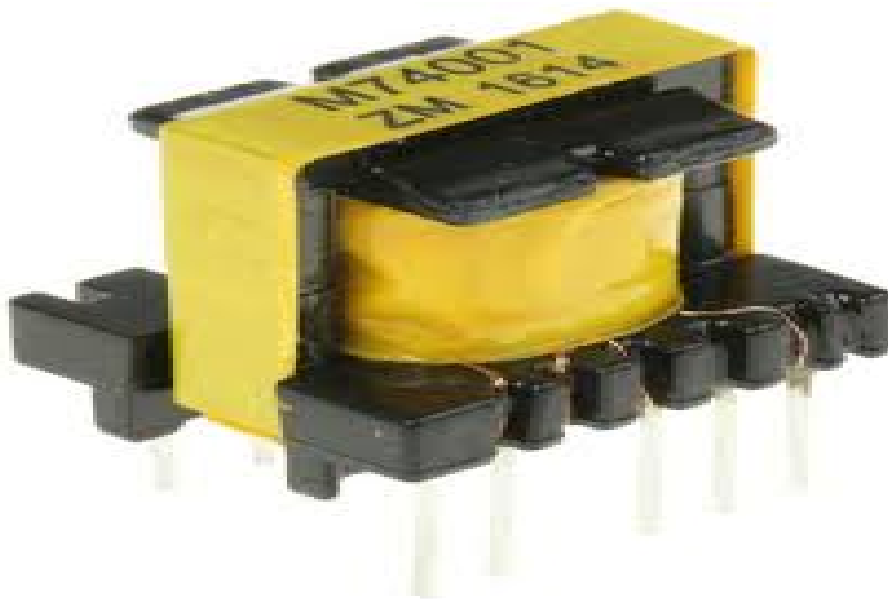


Figure 5.10: SMPS transformer

The first step in designing an SMPS transformer is to choose a core and bobbin geometry. Most practical SMPS transformer designs are derived from standard geometries offered by Ferro cube and other manufacturers. The decision of which geometry to choose is a function of many interrelated variables, and the discussion that follows will assist in this process. The amount of power deliverable through a given SMPS transformer is a function of output power and frequency. As the frequency increases, greater power can be accommodated with a given transformer core and bobbin, or possibly a smaller geometry core can be used. Figure A shows the typical RMS power available from a 10 W and a 1 kW SMPS transformer assuming the temperature rise of each transformer is fixed at 40° C.

For the high currents typical of low voltage applications above 2.5 kW, it becomes increasingly difficult to manage the AC winding losses. Compounding this problem, scaling effects dictate lower power densities for both the core and the bobbin, to prevent excessive temperature rise. Therefore higher power SMPS applications typically operate at lower frequencies. To some degree the problem of managing high frequency high current density power has been mitigated for the transformer designer because silicone devices such as IGBT's have current and frequency limits below what transformers can accommodate today.

Driver IC 4047

CD4047BMS consists of a gatable astable multivibrator with logic techniques incorporated to permit positive or negative edge triggered monostable multivibrator action with retriggering and external counting options. Inputs include +TRIGGER, -TRIGGER, ASTABLE, ASTABLE, RETRIGGER, and EXTERNAL RESET. Buffered outputs are Q, \bar{Q} , and OSCILLATOR. In all modes of operation, an external capacitor must be connected between C-Timing and RC-Common terminals, and an external resistor must be connected between the R-Timing and RC common terminals as shown in Fig 5.11

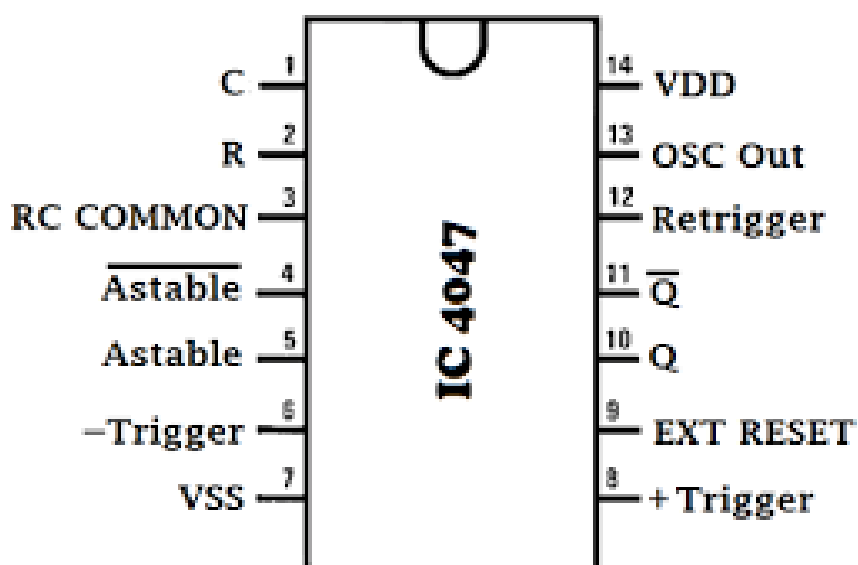


Figure 5.11: IC 4047

The astable operation is enabled by a high level on the astable input or a low level on the astable input, or both. The period of the square wave at the Q and \bar{Q} Outputs in this mode of operation is a function of the external components employed. “True” input pulses on the astable input or “Complement” pulses on the astable input allow the circuit to be used as a gatable multivibrator. The oscillator output period will be half of the Q terminal output in the astable mode.

However, a 50 percent duty cycle is not guaranteed at this output. The CD4047 triggers in the monostable mode when a positive going edge occurs on the +trigger input while the -trigger is held low. Input pulses may be of any duration relative to the output pulse. If re-trigger capability is desired, the re-trigger input is pulsed. The retriggerable mode of operation is limited to positive going edge. The

CD4047BMS will retrigger as long as the re-trigger input is high, with or without transitions. An external countdown option can be implemented by coupling “Q” to an external “N” counter and resetting the counter with trigger pulse. The counter output pulse is fed back to the astable input and has a duration equal to N times the period of the multivibrator.

A high level on the astable external reset input assures no output pulse during an “ON” power condition. This input can also be activated to terminate the output pulse at any time. For monostable operation, whenever VDD is applied, an internal power on reset circuit will clock the Q output low within one output period.

MOSFET

MOSFET (metal-oxide semiconductor field-effect transistor) as shown in Fig 5.12. is a special type of field-effect transistor (FET) that works by electronically varying the width of a channel along which charge carriers (electrons or holes) flow. The wider the channel, the better the device conducts. The charge carriers enter the channel at the source, and exit via the drain. The width of the channel is controlled by the voltage on an electrode called the gate, which is located physically between the source and the drain and is insulated from the channel by an extremely thin layer of metal oxide.

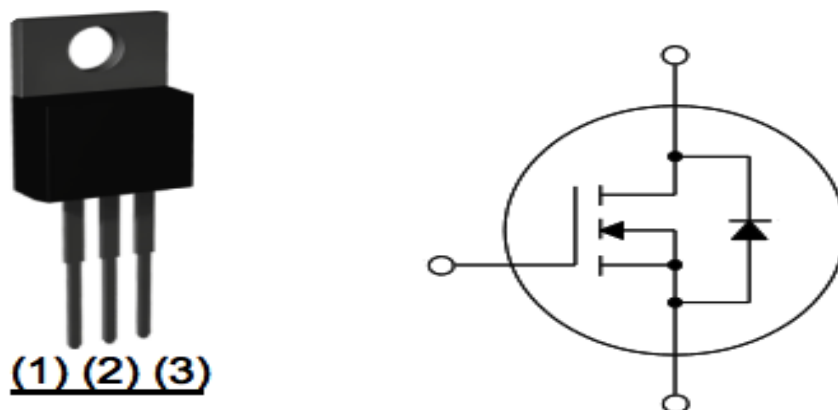


Figure 5.12: MOSFET

There are two ways in which a MOSFET can function. The first is known as depletion mode . When there is no voltage on the gate, the channel exhibits its maximum conductance . As the voltage on the gate increases (either positively

or negatively, depending on whether the channel is made of P-type or N-type semiconductor material), the channel conductivity decreases. The second way in which a MOSFET can operate is called enhancement mode . When there is no voltage on the gate, there is in effect no channel, and the device does not conduct. A channel is produced by the application of a voltage to the gate. The greater the gate voltage, the better the device conducts.

The MOSFET has certain advantages over the conventional junction FET, or JFET. Because the gate is insulated electrically from the channel, no current flows between the gate and the channel, no matter what the gate voltage (as long as it does not become so great that it causes physical breakdown of the metallic oxide layer). Thus, the MOSFET has practically infinite impedance . This makes MOSFETs useful for power amplifiers. The devices are also well suited to high-speed switching applications. Some integrated circuits (IC s) contain tiny MOSFETs and are used in computers.

5.3.2 Hardware Results

The prototype hardware setup of prototype model of PV-system is developed. This consists of solar panel, battery, charge controller circuit, boost converter, driver circuit, step up transformer and grid. The supply voltage 440V is taken as a grid voltage which is directly connected to the load. The solar system is integrated to the grid. For three phases three different driver circuits along with the transformer used and connected to three different loads. During the operation of without PV system the 440V supply is directly feed to the grid and the generated supply from the solar is also fed to grid. During this operation condition the solar inverter only performs the operation of converting DC to AC. The inverter performs the operation of PV system also during when inverter circuit is also get supply from the charge controller. Then at that condition the grid power increases.

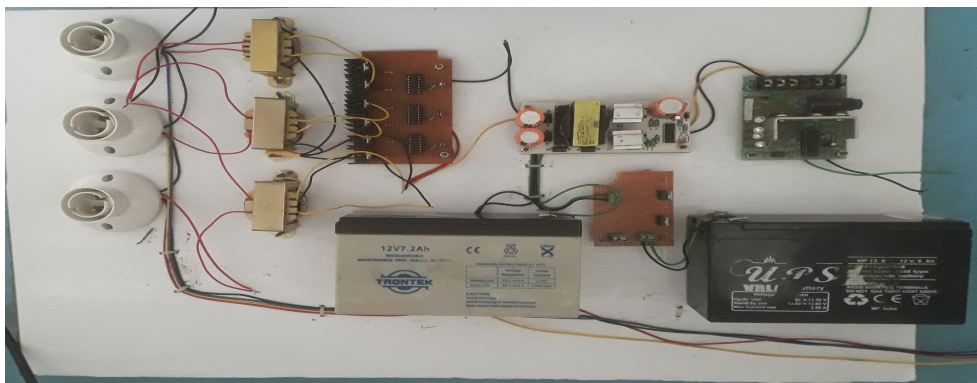


Figure 5.13: Prototype model

The grid power is also increase at that condition. The main component of driver circuit is the 4047 IC is the PWM generation IC. That generates the pulses for the operation of MOSFET. The output pin of 4047IC is connected to the gate of MOSFET. Then the MOSFETs output is 12V, connected to the transformer of range 12-0-12. That step up the voltage up to 230 volt. Similarly, this circuit is for other two phases. The charge controller is used to control the battery charging along with the MPPT. If the battery charges above the preset value then it generates low output and MOSFET gets off so that the battery is disconnected from the supply. Similarly, for discharging when the battery discharges below preset value then it disconnected the load from battery.

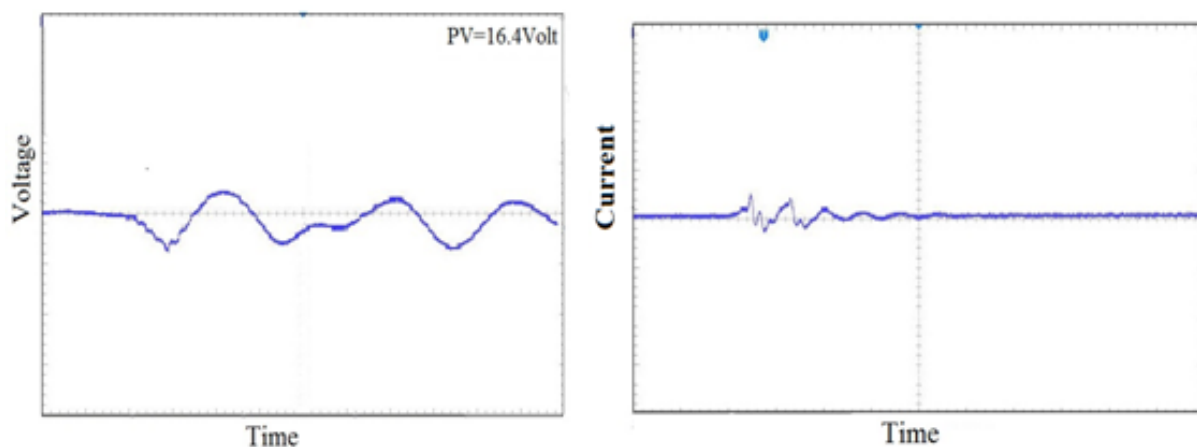


Figure 5.14: PV voltage and current

The solar output depends on solar irradiance and used in the quality of the material. The solar panel output is 16.2 volt DC and current is 0.5amp. The

maximum solar irradiance the output of the solar panel is maximum. the open circuit voltage is 24.2 volt and short circuit current is 0.64 amp, the prototype hardware in solar panel output voltage is produce in 16.2 volt DC and 0.3 amp current as shown in Fig. 5.14.

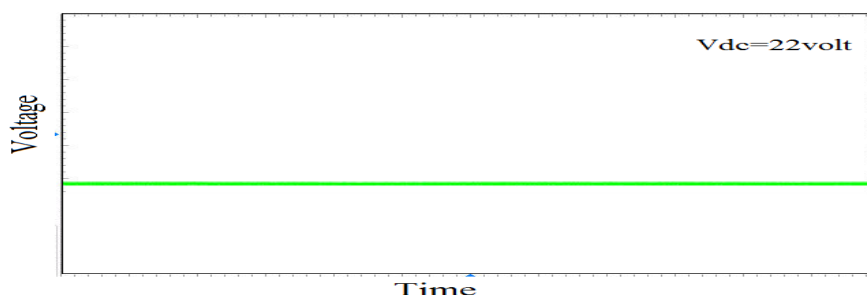


Figure 5.15: Boost converter output voltage

The boost converter is a specially designed converter this converter is input give from the solar side in 12 volt DC. This converter converts the 12 volt DC to 12 volt AC, this 12 volt AC is stepping up to 22 volt AC by using the isolating step-up transformer. This 22 Volt AC is again converted in 22 volt DC by using bridge rectifier as shown in Fig. 5.15.

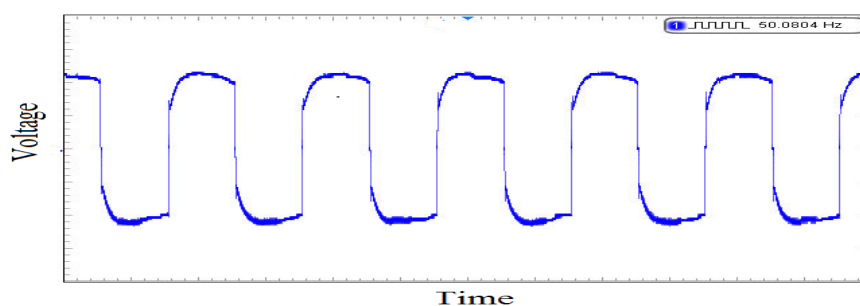


Figure 5.16: Inverter circuit output Voltage

The inverter function is converter the DC voltage to Ac voltage. The inverter input gives to boost converter side. The inverter circuit in the main component of the driver circuit is the 4047 IC is the PWM generation IC. That generates the pulses for the operation of MOSFET. Then the MOSFETs output is 12V AC as shown in Fig 5.16, connected to the transformer of range 12-0-12. That step up the voltage up to 230 volts. Similarly, this circuit is for the other two phases.

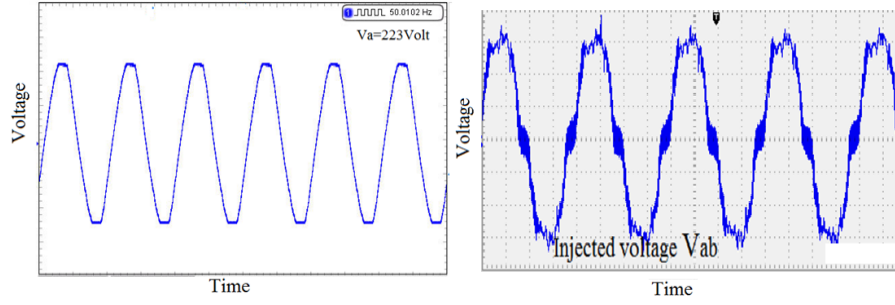


Figure 5.17: Injected voltage in grid connected mode V_{ab} Autonomous voltage

The grid is connected with the experimental result of the nature of different loads is given in fig.5.17. The grid connected mode in grid voltage $V_a b=415$ volt and grid current $i_a=4.2$ Amp. When there is a transfer Autonomous to grid connected mode, grid voltage is out of phase. This is seen as a huge current cause. A part of synchronizing Control means that the ON / OFF control is banned closed Current It is seen that the peak goes around the present 14A. $T_{total} = 30ms$ after the ON/OFF control, Turns off the converter. Transfer to Autonomous Mode to Grid mode image is displayed Fig.5.17 The case captures where the proposed synchronization control is not implemented. For better understanding of the current primary line 120/240V Transformer is caught.

5.4 Comparison

To determine the importance and uniqueness of the proposed framework, a comparison is made with other existing strategies that fall under the same employment goals. In implementing this approach, three approaches were used that were important: the hybrid voltage and the current strategy control, and droop control. Therefore, these methods were developed for comparison with the proposed model as shown in Table 5.1.

The configuration contains the current control structure and eliminates the need for an islanding algorithm that is represented by the first two rows of comparisons in the table. This minimizes the complexity of the not required algorithms in droop control method as compared to hybrid and indirect control. The hybrid and indirect control method is the same as the grading procedure regarding the complexity of the algorithm requirements.

The other four components of the comparison are a demonstration of the im-

Table 5.1: Comparison Table

Sr.No.	parameter	Hybrid control.	Indirect control.	Droop control.
1	Requirement of two separate controllers	Yes	Yes	No
2	Requirement of islanding algorithm	Yes	Yes	No
3	MPPT/Charging in grid connected mode	Yes	Yes	No
4	Uncontrolled state when transferring from grid connected mode to autonomous mode	Yes	No	No
5	Transient performance	Fast	Fast	Fast
6	PCC voltage and Frequency dependency on load	No	Yes	Yes
7	harmonic load cetering	Yes	No	No
8	Plug and play usage in microgrid	No	Yes	yes

plementation of price strategies. The proposed control and its adaptive ability of the switch to the regulator offer the advantage of using the highest power in the model derived from the source in a connected system.

This feature in the computation process is achieved without a standard mode detection algorithm. The combination of exercise and exercise also offers the same benefits. However, the cost of using a common data algorithm. This droop control offers what the power of the other system cannot. This control mechanism prevents the occurrence of an uncontrolled state when transferring from GC to AM.

The use of constraints due to its transition from one control to another during the transition is not free from this problem. The problem is that there is no problem with the use of the drop control and indirect control methods and it is similar to the configuration control in this section. All of the precautions are taken immediately in response to the exception except for the fall because skin control is based in a significant way.

The PCC voltage and load frequency dependence are a problem for droop control and indirect control its misuse. In the default setting, the frequency and voltage are limited to a limit or maximum in the AM.

This prevents critical loads which require precise frequency and voltage to be powered using this control. Catering non linear and harmonic loads in its base form is also a problem for both these controls as well. Thus it can be seen that with respect to the performance criteria, the proposed control emerges as a clear winner satisfying all the four parameters.

5.5 Closure

The simulation models along with its results are given in this section. Simulation models consist of proposed V-F and P-Q control techniques. The result of the proposed technique is compared with the hybrid and islanding algorithm. This chapter also consists of results of experimental setup of proposed.

Chapter 6

Future scope and Conclusion

6.1 Conclusion

The PV system is used to power capability improvement, reliability is increased, technical performance is improved; reduce the emission of house gases. The PV system is operated in autonomous mode/islanding mode and grid-connected mode. The requirement of renewable energy source is connected in a grid and operate is separate. The modern power system in an important task of renewable energy source is the integration and control of the grid. The proposed control strategy also provides a smooth transition the PV-side PQ control in grid connected mode on V-f control in island mode. This is the most important feature required in modern microgrid controllers. This is the most important component required in modern microgrid controllers. Integrated voltage and frequency (VF) and active and improved power (PQ) in the core of the microgrid are planning strategies for VSI. The three core micro-buses make the PQ gene-generator run at high power and support sharing working power based on VF distribution. This control method can check the power distribution between the VSI and the microgrid. The control module also provides a good change of PQ control over the PV side to a VF control offline communication system. Proper conversion of control from Vf to continuous control of compressive power and voltage across PV side and from continuous suppression of working power to continuous control to a diesel generator is proven to good results. . This helps the controller adjust to changes in height depending on the availability of the battery. The proposed V-f control method shows very satisfactory performance when restoring very low voltage and frequency to nominal

values in just 2 seconds. This is much faster than controlling a diesel generator, which takes about 10 seconds to calm down. Consequently, PV installations and batteries can be effectively used to recover micro-grid frequency and PCC voltage after disturbances. Similarly, the proposed integrated and coordinated P-Q control algorithm can be effectively used to provide some critical micro-grid loads with solar photovoltaic cells and batteries.

6.2 Future Scope

The proposed control strategy also provides a smooth transition of the PQ control on the PV side in the network connection to the VF control offline. Effective smooth conversion of controls from V-f to constant control of active power and voltage on the PV side and from constant control of active power to frequency control in a diesel generator is confirmed with satisfactory results. This feature helps the controller adjust to changing light levels based on battery availability.

REFERENCES

- [1] E. I. Batzelis, “Simple pv performance equations theoretically well founded on the single-diode model,” *IEEE Journal of Photovoltaics*, vol. 7, pp. 1400–1409, Sep. 2017.
- [2] Y. Mahmoud and E. El-Saadany, “Accuracy improvement of the ideal pv model,” *IEEE Transactions on Sustainable Energy*, vol. 6, pp. 909–911, July 2015.
- [3] W. Xiao, F. F. Edwin, G. Spagnuolo, and J. Jatskevich, “Efficient approaches for modeling and simulating photovoltaic power systems,” *IEEE journal of photovoltaics*, vol. 3, no. 1, pp. 500–508, 2012.
- [4] B. C. Babu and S. Gurjar, “A novel simplified two-diode model of photovoltaic (pv) module,” *IEEE journal of photovoltaics*, vol. 4, no. 4, pp. 1156–1161, 2014.
- [5] A. M. S. S. Andrade, L. Schuch, and M. L. da Silva Martins, “Analysis and design of high-efficiency hybrid high step-up dc–dc converter for distributed pv generation systems,” *IEEE Transactions on Industrial Electronics*, vol. 66, pp. 3860–3868, May 2019.
- [6] F. M. Shahir, E. Babaei, and M. Farsadi, “Extended topology for a boost dc–dc converter,” *IEEE Transactions on Power Electronics*, vol. 34, pp. 2375–2384, March 2019.
- [7] X. Cheng, Y. Zhang, and C. Yin, “A family of coupled-inductor-based soft-switching dc–dc converter with double synchronous rectification,” *IEEE Transactions on Industrial Electronics*, vol. 66, pp. 6936–6946, Sep. 2019.
- [8] G. Diaz, C. Gonzalez-Moran, J. Gomez-Aleixandre, and A. Diez, “Complex-valued state matrices for simple representation of large autonomous microgrids supplied by pq and vf generation,” *IEEE Transactions on Power Systems*, vol. 24, pp. 1720–1730, Nov 2009.
- [9] N. Hajilu, G. B. Gharehpetian, S. H. Hosseinian, M. R. Poursistani, and M. Kohansal, “Power control strategy in islanded microgrids based on vf and pq theory using droop control of inverters,” in *2015 International Congress on Electric Industry Automation (ICEIA 2015)*, pp. 37–42, Feb 2015.

- [10] S. S and L. Umanand, “A unified controller for utility-interactive uninterruptible power converters for grid connected and autonomous operations,” *IEEE Transactions on Power Electronics*, vol. 34, pp. 3871–3887, April 2019.
- [11] S. Mansour, M. I. Marei, and A. A. Sattar, “Decentralized secondary control for frequency restoration of microgrids with vf and pq droop controlled inverters,” in *2017 Nineteenth International Middle East Power Systems Conference (MEPCON)*, vol. 2, pp. 1170–1176, Dec 2017.
- [12] S. Adhikari and F. Li, “Coordinated v-f and p-q control of solar photovoltaic generators with mppt and battery storage in microgrids,” *Smart Grid, IEEE Transactions on*, vol. 5, pp. 1270–1281, 05 2014.
- [13] Q. Li and P. J. Wolfs, “A review of the single phase photovoltaic module integrated converter topologies with three different dc link configurations,” *IEEE Transactions on Power Electronics*, vol. 23, pp. 1320–1333, 2008.
- [14] H. Nikkhajoei and R. H. Lasseter, “Distributed generation interface to the certs microgrid,” *Power Delivery, IEEE Transactions on*, vol. 24, pp. 1598 – 1608, 08 2009.
- [15] V. Gokul, S. Gomathi, and D. Venkatesan, “Powercontrol analysis of hybrid microgrid,” *International Journal of Research and Engineering*, vol. 2, no. 4, pp. 50–56, 2015.
- [16] M. M. R. Singaravel and S. A. Daniel, “Mppt with single dc–dc converter and inverter for grid-connected hybrid wind-driven pmsg–pv system,” *IEEE Transactions on Industrial Electronics*, vol. 62, pp. 4849–4857, 2015.
- [17] A. Tsikalakis and N. Hatziargyriou, “Centralized control for optimizing microgrids operation,” *IEEE Transactions on Energy Conversion*, vol. 23, pp. 241–248, 2008.
- [18] D. S. Ochs, B. Mirafzal, and P. Sotoodeh, “A method of seamless transitions between grid-tied and stand-alone modes of operation for utility-interactive three-phase inverters,” *IEEE Transactions on Industry Applications*, vol. 50, pp. 1934–1941, May 2014.
- [19] S. Hu, C. Kuo, and T. Lee, “Design of virtual inductance for droop-controlled inverter with seamless transition between islanded and grid-connected operations,” in *2012 IEEE Energy Conversion Congress and Exposition (ECCE)*, pp. 4383–4387, Sep. 2012.

- [20] R. Teodorescu and F. Blaabjerg, “Flexible control of small wind turbines with grid failure detection operating in stand-alone and grid-connected mode,” *IEEE Transactions on Power Electronics*, vol. 19, pp. 1323–1332, Sep. 2004.
- [21] S. Hu, C. Kuo, T. Lee, and J. M. Guerrero, “Droop-controlled inverters with seamless transition between islanding and grid-connected operations,” in *2011 IEEE Energy Conversion Congress and Exposition*, pp. 2196–2201, Sep. 2011.
- [22] A. G. Tsikalakis and N. D. Hatziargyriou, “Centralized control for optimizing microgrids operation,” in *2011 IEEE power and energy society general meeting*, pp. 1–8, IEEE, 2011.
- [23] H. Hu, S. Harb, N. Kutkut, I. Batarseh, and Z. J. Shen, “A review of power decoupling techniques for microinverters with three different decoupling capacitor locations in pv systems,” *IEEE Transactions on Power Electronics*, vol. 28, pp. 2711–2726, 2013.

LIST OF PUBLICATIONS ON PRESENT WORK

- [1] Patil Jaydeep J., Bhattar Chandrakant L., “AC Grid Connected PV System with Autonomous Operation using V(Q) and F(P) Control Strategy ”, International Conference on Intelligent Computing Instrument and Control technologies. 2019
- [2] Patil Jaydeep J., Bhattar Chandrakant L., “AC Grid Connected PV System with Autonomous Operation ”in review in ECTI transaction on Electrical Engineering, Electronics and Telecommunications, Thailand.

